Physiological and proteomic response of Escherichia coli O157:H7 to a bioprotective lactic acid bacterium in a meat environment

Alejandra Orihuel, Lucrecia Terán, Jenny Renaut, Sébastien Planchon, María Pía Valacco, Emilse Masias, Carlos Minahk, Graciela Vignolo, Silvia Moreno, André M. De Almeida, Lucila Saavedra, Silvina Fadda

PII: S0963-9969(19)30500-9
DOI: https://doi.org/10.1016/j.foodres.2019.108622
Article Number: 108622
Reference: FRIN 108622

To appear in: *Food Research International*

Received date: 11 April 2019
Revised date: 12 August 2019
Accepted date: 15 August 2019

Please cite this article as: A. Orihuel, L. Terán, J. Renaut, et al., Physiological and proteomic response of Escherichia coli O157:H7 to a bioprotective lactic acid bacterium in a meat environment, Food Research International, https://doi.org/10.1016/j.foodres.2019.108622

Physiological and proteomic response of *Escherichia coli* O157:H7 to a bioprotective lactic acid bacterium in a meat environment

Alejandra Orihuel[1], Lucrecia Terán[2], Jenny Renaut[4], Sébastien Planchon[4], María Pía Valacco[6], Emilse Masias[3], Carlos Minahk[3], Graciela Vignolo[1], Silvia Moreno[6], André M. De Almeida[5], Lucila Saavedra[2], Silvina Fadda[1,*] sfadda@cerela.org.ar

[1]Technology, Centro de Referencia para Lactobacilos, Consejo Nacional de Investigaciones Científicas y Técnicas (CERELA-CONICET), San Miguel de Tucumán, Tucumán, Argentina.

[2]Genetics, Centro de Referencia para Lactobacilos, Consejo Nacional de Investigaciones Científicas y Técnicas (CERELA-CONICET), San Miguel de Tucumán, Tucumán, Argentina.

[3]Instituto Superior de Investigaciones Biológicas (INSIBIO), CONICET-UNT, and Instituto de Química Biológica "Dr. Bernabé Bloj", Facultad de Bioquímica, Química y Farmacia, UNT. Chacabuco 461, T4000ILI – San Miguel de Tucumán, Argentina.

[4]LIST - Luxembourg Institute of Science and Technology "Environmental Research and Innovation" (ERIN) department, Belvaux, Luxemburg.

[5]Instituto Superior de Agronomia, University of Lisbon, Lisbon, Portugal.

[6]Instituto de Química Biológica de la Facultad de Ciencias Exactas y Naturales (IQUIBICEN), CONICET Universidad de Buenos Aires, Buenos Aires C1428EGA, Argentina

[*]**Corresponding author.**

Abstract

The enterohemorrhagic *Escherichia (E.) coli* (EHEC) is a pathogen of great concern for public health and the meat industry all over the world. The high economic losses in meat industry and the high costs of the illness highlight the necessity of additional efforts to control this pathogen. Previous studies have demonstrated the inhibitory activity of *Enterococcus mundtii* CRL35 towards EHEC, showing a specific proteomic response during the co-culture. In the present work, additional studies of the EHEC-*Ent. mundtii* interaction were carried out: i) differential protein expression of *E. coli* O157:H7 NCTC12900 growing in co-culture with *Ent. mundtii* in a meat environment, ii) the reciprocal influence between these two microorganisms in the adhesion to extracellular matrix (ECM) proteins and iii) the possible induction of the

phage W933, coding for Shiga toxin (Stx1), by *Ent. mundtii* CRL35. Proteomic analysis showed a significant repression of a number of *E. coli* NCTC12900 proteins in co-culture respect to its single culture, these mostly related to the metabolism and transport of amino acids and nucleotides. On the other hand, statistically significant overexpression of EHEC proteins involved in stress, energy production, amino acid metabolism and transcription was observed at 30 h respect to 6 h when EHEC grew in co-culture. Data are available via ProteomeXchange with identifier PXD014588. Besides, EHEC showed a decreased adhesion capacity to ECM proteins in the presence of the bioprotective strain. Finally, *Ent. mundtii* CRL35 did not induce the lytic cycle of W933 bacteriophage, thus indicating its potential safe use for eliminating this pathogen. Overall, this study expands the knowledge of EHEC- *Ent. mundtii* CRL35 interaction in a meat environment, which will certainly contribute to find out effective biological strategies to eliminate this pathogen.

Keywords

Enterohemorrhagic *Escherichia coli* (EHEC), Bioprotective cultures, Meat safety, Bacterial interaction, Proteomics.

1. Introduction

In recent years, the infections with enteric pathogens have been the major short-term health risks associated to meat consumption. Indeed, *Campylobacter*, *Salmonella*, and pathogenic *E. coli* colonize the gastrointestinal tracts of a wide range of wild and domestic animals, especially animals raised for human consumption.

Shiga toxin-producing *E. coli* (STEC) emerged as a quite significant foodborne pathogen because of the severe consequences of its potent Shiga toxins, low infection dose and acid tolerance (Hussein & Bollinger, 2005). Although many food and dairy products may act as vectors, the majority of the reported cases have been linked to the consumption of foods of bovine origin, with ground beef being the most frequently identified source. Consequently, STEC is a major concern for the sustainability of the meat industry and a serious threat to public health (Rangel, Sparling, Crowe, Griffin, & Swerdlow, 2005).

Shiga toxins (Stx) are encoded by Lambda type prophages (933W and 933J) in *E. coli* O157: H7 (O'Brien et al., 1984). These prophages are integrated into the bacterial chromosome in a lysogenic state and the activation of their lytic cycle leads to the production of Stx, which are then released during cell lysis (Johansen, Wasteson, Granum, & Brynestad, 2001) upon activation of the bacterial SOS response (Walker, 1996). Multiple environmental signals regulate the expression of Stx, such as temperature, growth phase, antibiotics, reactive oxygen species (ROS), quorum sensing signals, iron concentration, etc. The expression, regulation and mechanism of action of this toxin have been the subject of intensive studies over the last decades. If we understand how this system works and how it can be modulated we may develop new strategies to counteract its effect and prevent diseases (Sperandio & Pacheco, 2012). Interestingly; in some Hemolytic Uremic Syndrome (HUS) outbreaks live bacteria were not found in the food samples (Goh et al.,

2002), indicating that the Shiga toxins would be the agents that triggered the outbreak. Weeratna & Doyle (1991) have shown that the inoculation of Enterohemorrhagic *Escherichia coli* (EHEC) in foods produces high levels of Shiga toxin in milk (306 ng / mL) and meat (452 ng / mL).

On the other hand, meat can be contaminated with bacteria during slaughter and the subsequent processing, and attachment of *E. coli* O157:H7 to beef has been reported. In fact, the Extracellular Matrix of muscle fibers (ECM) seems to be involved in bacterial attachment to meat surfaces (Chagnot et al., 2013, 2017; Chen, Rossman, & Pawar, 2007; Giaouris, 2015; Rivas, Dykes, & Fegan, 2006). Studying the interactions between ECM and bacteria could result in more targeted interventions to improve meat safety and quality. Moreover, it is crucial to understand how *E. coli* O157 interacts with other microorganisms since it will allow the development of effective strategies to inactivate this pathogen.

In the present work, different aspects of the response of *E. coli* O157:H7 during the interaction with a bioprotective Lactic Acid Bacteria (LAB) strain in meat environments were analyzed. Differential protein expression of EHEC in pure or mixed cultures and adhesion to ECM proteins was studied. Such analyses are important for gaining insight into the competitive advantages of the bioprotective strain during meat adhesion and colonization. In addition, assays were carried out to evaluate the possible induction of the *E. coli* phage W933 by *Ent. mundtii* CRL35 in order to know how safe its use as bioprotective culture to control EHEC in meat may be.

2. Materials and methods

2.1 Bacterial strains and culture conditions

The atoxigenic *Escherichia coli* O157:H7 NCTC12900 (National Type Culture Collection, Colindale, London), kindly provided by Dr. R. R Raya (CERELA CONICET), was selected as the pathogen model. *E. coli* NCTC12900 was isolated in Austria in 1992 and does not produce enterotoxins Stx1 nor Stx2 (Dibb-Fuller, Best, Stagg, Cooley, & Woodward, 2001; Best et al., 2003). The genome information of this strain is available at the European Nucleotide Archive with the following Accession Number (AN): ERS1324157, and in the National Center for Biotechnology Information (NCBI) with the AN: UFZH00000000.1 (https://www.ncbi.nlm.nih.gov/nuccore/UFZH00000000.1/). This strain was kept at −80 °C in LB (Luria

Bertani) medium in the presence of 20 % (v/v) glycerol as cryoprotectant. To obtain fresh cultures, the *E. coli* strains were transferred twice to LB broth. Cells were cultured at 37 °C for 8 h, in the first incubation, and 16 h in the second incubation.

Enterococcus mundtii CRL35 strain of cheese origin, has been deposited in the CERELA culture collection under the AN: CRL35. The genome of this strain was sequenced and deposited under the following AN: JDFT00000000 (Bonacina, Saavedra, Suárez, & Sesma, 2014). Fresh cultures were obtained from freeze-dried stocks and transferred twice to MRS broth (Merck, Buenos Aires, Argentina) incubated at 30 °C for 24 h and used for further inoculations. The stock culture was stored at -80°C in milk yeast medium (10 % w/v skim milk, 0.5 % w/v yeast extract) containing 10 % (v/v) glycerol as cryoprotectant.

The strain *E. coli* C600Δtox (National Academy of Medicine, USA) was kindly provided by Dr. Alison A. Weiss (Department of Molecular Genetics, Biochemistry & Microbiology, University of Cincinnati, Ohio, USA). The strain has the *stx2* gene replaced by the green fluorescence protein encoding gene (ϕΔTOX:GFP) by means of allelic exchange. This strain was used to evaluate phage cycle induction by the bioprotective strain, *Ent. mundtii* CRL35.

The strain designated *E. coli* B, a clonal descendant of *Bacillus coli* (Coli Genetic Stock Center, CGSC collection) (Daegelen, Studier, Lenski, Cure, & Kim, 2009) was used for titration assays as a sensitive strain to W933 phage.

2.2 Sarcoplasmic Model System

The sarcoplasmic model system (SMS) chosen for studying EHEC- *Ent. mundtii* interaction was prepared as previously described Fadda, Vignolo, Holgado, & Oliver (1998) with some modifications. Briefly, 10 g of bovine *semimembranosus* muscle was homogenized with 100 mL of deionized water for 8 min in a Stomacher 400 blender (Stomacher, London, UK). After centrifugation of the homogenate (14,000 *g*, 20 min at 4 °C), the supernatant containing sarcoplasmic proteins and other soluble compounds was filtered through Whatman paper, filter-sterilized through a 0.22 µm-pore-size filter (Steritop GP, Biopore, Buenos Aires, Argentina) and supplemented with 0.5 % glucose and 0.01 % Tween 80. The sterility of the system was confirmed by plating in Plate Count Agar (PCA) (Fig. S1).

2.3 Proteomics study

For differential proteomic analysis, the interaction between EHEC and *Ent. mundtii* CRL35 was studied in SMS cultures by means of two dimensional electrophoresis (2DE), as described by Orihuel et al. (2018b). Two different time points during the bacterial growth were evaluated: T1, corresponding to 6 h of growth when both microorganisms (*Ent. mundtii* CRL35 and *E. coli* NCTC12900) were in the exponential growth phase, and T2 that corresponds to 30 h (stationary and death phases for *Ent. mundtii* and *E. coli* during co-culture, respectively). To reach the death phase for pure cultures of *E. coli*, 96 h were needed (Orihuel et al., 2018b).

2.3.1 Cell recovery for proteomic analyses

E. coli O157:H7 NCTC12900 (10^4 CFU/mL) was grown alone and in co-culture with *Ent. mundtii* CRL35 (10^6 CFU/mL) , in 100 mL of SMS. Cells from co-cultures were harvested at T1 and T2. Cells from *E. coli* and *Ent. mundtii* growing alone at T1 and T2, were collected separately. Cells from different cultures were harvested by centrifugation at 8,000×g for 10 min at 20 °C, washed with 0.1M Tris-HCl buffer, pH 7.5 and centrifuged again at 8,000 ×g for 10 min at 20 °C. The resulting pellets were stored at −20 °C until protein extraction. Three independent biological replicates were performed for each condition (Fig. S1).

2.3.2 Preparation of cell free protein extracts for proteomic analysis

This protocol was described in detail by Orihuel et al. (2018b). Briefly, when individual cultures were assessed, *Ent. mundtii* and *E. coli* cell pellets harvested at T1 were mixed before lysis and the same strategy was applied for T2 samples. These mixtures were called synthetic mixtures (SM). This procedure was carried out to standardize and avoid differences in cell lysis efficiency between mono and co-cultures, as well as problems derived from differences in protein enrichment of each microorganism in 2DE gels, that could affect proteome comparisons. The cell proportions of each microorganism used for T1 and T2 mixtures, coming from single cultures, were established according to the cell counts obtained in the respective co-culture in order to have in the mix a similar ratio between the two microorganisms. In this way, it was ensured that the 600 µg of proteins loaded in the IPG strip, had the same protein proportion of each microorganism than in IPG strips loaded with samples from the co-culture. Each of these synthetic mixtures

(SM) will constitute the respective controls (single culture) at T1 and T2. The SM pellets as well as those pellets from co-cultures were mixed with glass beads (150-212 μm diameter, Sigma-Aldrich Co., St. Louis, MO, USA) and 0.1M Tris-HCl buffer, pH 7.5 in a 1:2:1 (cell:buffer:bead) ratio. Then, cells were disrupted using a Mini-BeadBeater-8 cell disrupter (Biospec Products Inc., Bartlesville, OK, USA) at maximum speed for 10 min (10 cycles of 1 min each, with 1-min intervals where samples were kept on ice). Cell debris, unbroken cells and glass beads were removed by centrifugation (14,500 ×g, 5 min, 15 ºC), and the cell-free supernatant were kept at-80ºC for proteomic analysis. The protein concentration of the extracts was estimated by the Bradford assay using bovine serum albumin as a standard (see Figure S1 for details of the whole procedure).

2.3.3 Two-dimensional gel electrophoresis (2DE)

Sample preparation and 2DE gels were carried out as previously described Bustos et al.(2015). Briefly, 600 μg of proteins were placed in each immobilized pH gradient (IPG) strip (Immobiline DryStrip Gels, linear pH 4-7, 18 cm, GE Healthcare; Uppsala, Sweden) and Isoelectrofocusing (IEF) was performed in Ettan IPGphor 3 (GE Healthcare, Uppsala, Sweden) at 53,500 Vh. For the second dimension, IPG strips were equilibrated at room temperature in 6 M urea, 2 % SDS, 30 % glycerol, 50 mM Tris-HCl, pH 8.0, containing alternatively 50 mM DTT (15 min) and then 400 mM iodoacetamide (15 min in the dark). Second dimension was performed on homogeneous 12.5 % polyacrylamide gels at the constant current of 15 mA/gel at 15 ºC (approximately 16 h) using an Ettan DALTsix Large Vertical System (GE Healthcare, Uppsala, Sweden). Gels were stained with colloidal Coomassie blue Stain according to Candiano et al. (2004), distained with distilled water. The 2DE maps were digitalized using Image Scanner III LabScan 6.0 (GE Healthcare, Uppsala, Sweden).

2.4 Image acquisition and data analysis

Volume spot quantization and normalization were performed on digitalized gel images (600 dpi) using the software Prodigy SameSpots version 1.0.3400.25570 (Totallab, Newcastle, UK). The volume of each spot was calculated and normalized by referring the values to the sum of total spot volumes within each gel. Student test for unpaired samples was applied. A protein was considered as differentially abundant if the

mean normalized spot volume varied at least 1.5-fold between compared spots. The effect was confirmed by analysis of variance at a significance level of $p<0.05$. Protein spots showing significant variations between the different conditions were manually excised from the gels using a scalpel blade and identified using mass spectrometry.

2.5 Mass spectrometry protein identification

Mass spectrometry analysis was carried out at LIST - Luxembourg Institute of Science and Technology "Environmental Research and Innovation" (ERIN) (spots selected after analyses I and II, Table 1) and at CEQUIBIEM (Facultad de Ciencias Exactas y Naturales, UBA, IQUIBICEN, CONICET, Buenos Aires, Argentina) (spots selected after analysis III, Table 2). Excised spots were subjected to tryptic digestion as previously described (Nally et al., 2017). After extraction with 50% (v/v) acetonitrile (ACN) containing 0.1% (v/v) trifluoroacetic acid (TFA), the peptides were dried by speed-vac at 50°C, mixed with 0.7 µL of 7 mg/mL α-cyano-4-hydroxycinnamic acid in 50% (v/v) ACN containing 0.1% (v/v) TFA and spotted on MALDI-TOF target plates.

Samples processed at LIST were analysed using a MALDI TOF/TOF™ 5800 (AB SCIEX, RedwoodCity, CA, USA) as follows: Spectra were obtained in positive reflectron mode, within a mass range of 900-4000 m/z. The positive-ion mass spectra were internally calibrated using the known trypsin auto-digestion peaks, when possible, or externally calibrated using the Mass Standards Kit for Calibration of AB SCIEX TOF/TOF™ Instruments (AB SCIEX, RedwoodCity, CA, USA). For each spot, the 10 most intense peaks of the MS spectrum were selected for MS/MS acquisition. Peak lists generated from all spectra of each spot were submitted, using ProteinPilot (v4.0, AB SCIEX, RedwoodCity, CA, USA), to a Mascot server in-house purchased (v2.4.2, Matrix Science, Boston, MA). Searches were carried out against NCBInr (20151110) database, taxonomy: *E. coli* for *E. coli* O157:H7 NCTC12900 samples, and against a database of all *Ent. mundtii* entries from the NCBInr (20160609, 20613 sequences) for *Ent. mundtii* CRL35 samples. The database search parameters were: peptide mass tolerance of 100 ppm, fragment mass tolerance of 0.5 Da, two missed cleavage, oxidation of methionine and tryptophan to kynurenin as variable modifications, and carbamidomethylation of cysteine as fixed modification. Only matched proteins with significant scores ($P< 0.05$) were considered.

Samples processed at CEQUIBIEM were analysed with an Ultraflex II Bruker Daltonics UV-MALDI-TOF-TOF mass spectrometer, equipped with a Nd:YAG laser (λ_{em} 355 nm) Spectra were obtained in positive reflectron mode, within a mass range of 800-4000 m/z. The positive-ion mass spectra were calibrated externally using the Bruker Peptide Calibration Mix Standard II (Bruker Daltonics PN222570). The generated spectra were visualized and compared with Flex Analysis 3.3 software. The generated peak list was based on signal-to-noise filtering and a contaminant exclusion list. Two high S/N MS peaks per sample were selected for fragmentation by MALDI TOF-TOF. MS and MS/MS spectra for each spot were combined using BioTools software (Bruker Daltonics). The resulting file was then searched using Mascot (Matrix Science, Boston, MA) against NCBInr (20160618) database, taxonomy: *E. coli* for *E. coli* O157:H7 NCTC12900 samples, and against the Mascot taxonomy category "Other firmicutes" for *Ent. mundtii* CRL35 samples. The database search parameters were: peptide mass tolerance of 100 ppm, fragment mass tolerance of 0.5 Da, one missed cleavage, oxidation of methionine as variable modifications, and carbamidomethylation of cysteine as fixed modification. Only matched proteins with significant scores ($P< 0.05$) were considered.

2.6 Functional analysis and interaction of proteins

The functional study of identified proteins and their classification into functional categories were performed using the databases UniProt, COGNITOR and Operon-Mapper to identify Clusters of Orthologous Groups of proteins (COGs) (Galperin, Makarova, Wolf, & Koonin, 2015; Taboada, Estrada, Ciria, & Merino, 2018).

To explore the interactions between the proteins that have shown differential expression at the same condition, we conducted an *in-silico* analysis using the publicly available STRING database (Search Tool for the Retrieval of Interacting Genes/Proteins), version 10.05 (Szklarczyk et al., 2015). For each set of differentially expressed proteins, the number of protein-protein interactions documented in the database was determined. A confidence level of 0.4 was selected and all the prediction methods available in STRING were used: known interactions of cured databases, experimentally determined interactions, and interactions predicted by neighboring genes, gene fusion, gene co-occurrence and others, such as based on bibliography, co-expression and protein homology (Szklarczyk et al., 2015). Therefore, we were allowed to build networks

where each protein was linked with the rest of the proteins differentially expressed in the same condition. The results obtained from this database were incorporated into the free Cytoscape version 3.6.1 software (Shannon et al., 2003), where the proteins represented by nodes also showed the fold change between different conditions evaluated.

2.7 Adhesion to extracellular matrix proteins

The adhesion of *Ent. mundtii* CRL35 and EHEC to the ECM proteins collagen IV (C6745, Sigma Aldrich) and laminin (L2020, Sigma Aldrich) has been studied following described methodology (Chagnot et al. 2013). For surface coating, a 50 µg/mL stock solution of each protein was prepared in 0.1 M carbonate buffer, pH 9.6. Then, 250 µL of these solutions were poured into the wells of 96-well plates. For nonspecific binding control, 250 µL of 1% bovine serum albumin solution was used instead for treating the wells. Plates were left overnight at 4 °C to allow proteins to become attached to the well surfaces. Afterwards, wells were washed three times with 200 µL PBST buffer (PBS buffer + 0.05% Tween 80) and then saturated with 250 µL 1% BSA en PBST. Suspensions of either *Ent. mundtii* CRL35 or EHEC (10^8 CFU/ml) were prepared from mid-exponential phase cultures and treated with 90 µg/mL chloramphenicol in order to prevent *de novo* protein synthesis and bacterial growth during the time frame of the assay. When microorganisms were tested individually, 200 µL of the bacterial suspensions were pipetted into the wells. However, when mixed suspensions were studied, 100 µl of each suspension was added to the wells in order to have the same final volume. Plates were incubated 2 h at 30 ºC, wells were then washed three times with tryptone water. Bacteria detached after treating wells with 250 µl 0.05% Triton X-100 for 30 min at room temperature. Aliquots of 100 µL were taken, serially diluted, plated on either MRS or LB plates, and finally colonies of *Ent. mundtii* CRL35 and EHEC were counted 48 and 24 h later, respectively. Cell counts were expressed as log CFU/mL. The percentages of adhered cells were calculated taking into account the total cells that were seeded at the beginning of the experiment. Each condition was evaluated in three independent assays carried out in triplicates.

2.8 Induction of the *E. coli* phage W933 by *Ent. mundtii* CRL35

Firstly, the optimal concentration of ciprofloxacin used for inducing the lytic cycle was studied. *E. coli* C600Δtox was grown in LB medium supplemented with 10 mM $CaCl_2$ at 37 °C until OD_{600nm} of 0.1. Afterwards, the culture was divided in 5 tubes and ciprofloxacin was added to each one to reach different concentrations: 7.5, 15, 30, 60 and 120 ng/ml. Cultures were further incubated at 37 °C until clear lysis was achieved.

If *Ent. mundtii* CRL35 is thought to be applied in meat preservation for antagonizing enterohemorrhagic *E. coli* counts, it has to be absolutely unable to induce the lytic cycle of 933-like phages (W933 in C600Δtox strain). In order to verify this phenomenon, the induction was carried out as described by Gamage, Strasser, Chalk and Weiss (2003) with minor modifications. Briefly, once cultures reached OD_{600nm} 0.1 as described above, they were divided in three tubes: a) a positive control of induction with the optimal concentration of ciprofloxacin, b) a tube containing *Ent. mundtii* CRL35 (final counts of 10^7 UFC/mL), c) a negative control of no induction. Cultures were further incubated for 24 h at 37 °C, taking samples at different time points where bacterial viability was assessed for *Ent. mundtii* and *E. coli* using MRS agar and Mac Conkey (Britania, Buenos Aires, Argentina) agar plates respectively. Plates were incubated at 30 °C during 48 and 24 h respectively. In addition, extra samples were taken from the induction cultures at 4 and 24 h, cells were pelleted by centrifugation and the phage-containing supernatants were filtered through sterile 0.22 µm filters and kept at 4 °C until phage titration.

For this purpose, the sensitive strain designated *E. coli* B was grown in LB medium until OD_{600nm} 0.5. Then, it was used to inoculate molten LB soft agar medium containing 10 mM $CaCl_2$ (0.7% agar kept at 45 °C). The soft agar was then spread onto regular LB agar plate. Finally, serial dilutions of the phages-containing supernatants were prepared and each dilution (5µL) was spotted onto the *E. coli* B lawn. Plates were incubated overnight at 37°C and lysis plaques were visually counted, the plaque forming units (PFU) per milliliter was calculated as follow:

PFU/mL = number of lysis plaques/inoculum volume x dilution

2.9 Statistical analyses

The experiments were carried out at least three times, and the values and the standard error were calculated from the data with three replicates. One-way analysis of variance with t-test was conducted, considering a *p* value of less than 0.05 as a statistically significant difference.

The hypergeometric distribution was assayed to evaluate the enrichment of COG categories that were determined with COGNITOR and the web platform Operon Mapper (Galperin, Makarova, Wolf, & Koonin, 2015; Taboada, Estrada, Ciria, & Merino, 2018). This allowed to relate the differentially expressed proteins of *E. coli* NCTC12900 in the different proteomic analysis in relation with the whole set of proteins encoded by this strain.

3. Results

3.1 Differential protein expression of *E. coli* NTCC12900 in co-culture with *Ent. mundtii* CRL35 in Sarcoplasmic Model System

In order to get a deeper understanding on the molecular response of *E. coli* NCTC12900 during the interaction with *Ent. mundtii* CRL35 in a meat environment, differential protein expression was evaluated according to the following comparisons: Analysis I: *E. coli* growing in co-culture versus *E. coli* growing individually at T1; Analysis II: *E. coli* growing in co-culture versus *E. coli* growing individually at T2 and Analysis III: *E. coli* growing in co-culture at T1 versus *E. coli* growing in co-culture T2 (Fig. S1). Representative 2DE maps of the proteomes when bacteria grew alone or in co-cultures are depicted in Fig. 1.

In the three proteomic analysis, protein spots showing the most significant differences in expression ($p<0.05$, fold>1.5) were submitted to MS/MS_based identification. From 106 spots, a total of 86 proteins were successfully identified, 41 belonged to *Ent. mundtii* (Orihuel et al. 2018b) and 45 to *E. coli* according to the respective protein databases. The present work was focused in proteins related to the *E. coli* proteome.

3.1.1 Differential protein expression of *E. coli* O157:H7 NCTC12900 growing alone or in co-culture

When proteomes from *E. coli* grown in co-culture were compared to proteomes from *E. coli* cells that have grown alone in the SMS, 32 proteins were differentially expressed at T1 and T2. In the co-culture at T1, eleven proteins were under-regulated showing between 1.7 to 2.5 fold change expression. Five of them were

related to amino acid metabolism (5-methyltetrahydropteroyltriglutamate homocysteine S-methyltransferase, cystathionine gamma-synthase, dihydroxy-acid dehydratase, 3-isopropylmalate dehydratase large subunit, arginine ABC transporter periplasmic binding protein) (45.6%). Additionally, two proteins were associated to nucleotide metabolism (carbamoyl-phosphate synthase- small subunit, inosine-5'-monophosphate dehydrogenase) (18.2%). One protein related to translation (elongation factor G) (9.1%), one involved in protein folding and processing (peptidylprolyl isomerase) (9.1%), one protein associated to transcription (transcription termination /antitermination protein) (9.1%), and one related to energy production and conversion (acetate kinase) (9.1%) (Table 1, Table S1, Fig. 2a). On the other hand, 19 proteins were also under-expressed in co-culture in respect to individual culture at T2 (2.0 - 6.1 fold change), whereas only two proteins were detected in higher amounts during co-culture at this time point. From the 19 repressed proteins, 6 were involved in amino acid metabolism (serine hydroxymethyl transferase, aminopeptidase N, glutamine synthase, cystathionine gamma synthase and 5 spots that were assigned to glutamate decarboxylase, encoded by different genes such as *gadA* and *gadB*) (33.3%). Two repressed proteins were related to translation (leucine-tRNA ligase and phenylalanine-tRNA ligase beta subunit) (10.5%), 2 involved in folding and processing (molecular chaperone DnaK) (10.5%), 2 related to stress (catalase/peroxidase and iron uptake system component) (10.5%), 2 involved in transport (taurine ABC transporter periplasmic binding protein and outer membrane Porin C) (10.5 %). One protein related to energy production and conversion (dihydrolipoyllysine-residue succinyltransferase component of 2-oxoglutarate dehydrogenase complex) (5.3%), one protein devoted to carbohydrate metabolism and transport (glyceraldehyde-3-phosphate dehydrogenase I type) (5.3%) and one protein related to secondary metabolite catabolism (taurine dioxygenase) (5.3%) showed also lower abundances (Table 1, Table S1, Fig. 2b). On the other hand, serin hydroxymetyl transferase, which is related to amino acid metabolism and dihydrolipoyllysine-residue succinyltransferase from the 2-oxoglutarate dehydrogenase complex, related to energy production and conversion, were the only two proteins overexpressed by *E. coli* during the co-culture (Table 1, Table S1). In summary, the amino acid metabolism proved to be highly repressed in co-cultured *E. coli* as compared to the levels of expression observed in *E. coli* growing as pure culture. This trend was found not only at 6 h but also at 30 h. Interestingly, a lower expression of proteins related to nucleotide metabolism was also observed at T1.

When performing a hypergeometric distribution to evaluate the probabilities of obtaining a certain COG category in our sample in relation with the ones encoded by the whole cell, many functional categories resulted to be enriched (Fig. S2 a, b, c). The categories corresponding to aminoacid (E) and nucleotides (F) transport and metabolism were the most significantly enriched during the proteomic analysis I: co-culture vs single culture at T1, because whilst it was more probable to find one protein related to E and none related to F categories, we found 5 and 1 proteins respectively, expressed differentially (Fig. S2a; Table 1, Table S1). On the contrary, the category related to general function prediction only (R) resulted impoverished because we found only 1 related protein while the expected probability was to find 2 (Fig. S2a; Table 1, Table S1). When the analysis II was carried out (co-culture versus individual culture at T2), categories E (amino acid transport and metabolism) and P (inorganic ion transport and metabolism) were among the most enriched. While categories G (carbohydrate transport and metabolism) and M (cell wall structure and biogenesis and outer membrane) resulted as expected: 1 found and 1 expected by the hypergeometric distribution (Fig. S2b, Table 1, Table S1).

3.1.2 Differential protein expression of *E. coli* O157:H7 NCTC12900 growing in co-culture at T2 versus T1

When the protein expression of *E. coli* NCTC12900 growing in co-culture was compared at the two different physiology states (T2 and T1), 13 identified proteins were differentially overexpressed ($p<0.05$; 1.8-2.5 fold change) at T2 respect to T1. These proteins were involved in different functional categories: energy production and conversion (malate dehydrogenase, formate C-acetyltransferase 1, phosphate acetyltransferase) (23.1%), stress (chaperone ClpB, molecular chaperone HtpG, catalase HPI) (23.1%); amino acid metabolism (glutamate decarboxylase; 2,3,4,5-tetrahydropyridine-2,6-dicarboxylate N-succinyl transferase) (15.4%), transcription (transcriptional repressor for purine, aerobic respiration control protein) (15.4%), carbohydrate metabolism and sugar transport (phosphoenolpyruvate phosphotransferase) (7.7 %), nucleotide metabolism (CTP synthase) (7.7%), cell wall biosynthesis (glucans biosynthesis protein G) (7.7%) (Table 2, Table S2, Fig. 2c). *E. coli* during the co-culture with *Ent. mundtii* CRL35 at 30 h was going through its death phase. Therefore, it was not surprising to find that the overexpressed proteins at this

condition were mostly involved in stress and energy production as an attempt to endure the hostile environmental conditions established by the competitive presence of *Ent. mundtii*.

When the hypergeometric analysis was carried out for proteins differentially expressed by EHEC in co-culture at T2 versus T1 (proteomic analysis III) many categories resulted enriched (C, K, O, T, F, E and P), specially energy production and conversion (C), molecular chaperones and related functions (O) and inorganic ion transport and metabolism (P) because we found 3 for C, 2 for O and 2 for P categories, while 1 or none was expected by the hypergeometric distribution. On the other hand, the G category was not modified because it was found 1 protein among our sample, as was exactly expected by this hypergeometric analysis. On the contrary for general functional prediction only (R) it was more probable to find two, and we found only one. This could imply an impoverishment of this category (Fig. S2c; Table 2, Table S2).

3.1.3 Functional analysis and interaction of proteins

Although the identified proteins were classified according to different functional categories, it is necessary to know whether the specific biological function of each protein relates to the others, and from there infer about the possible stimulation or inhibition of a given event, process or metabolism. Protein-protein interaction networks were build using both STRING v10.05 and Cytoscape v3.6.1 software (Fig. 3, Fig. 4 and Fig. 5): i) proteins repressed in EHEC in co-culture compared to the expression level seen in EHEC that grew alone, at T1 (Analysis I) (Fig. 3a and b); ii) proteins repressed in EHEC in co-culture compared to the expression level seen in EHEC that had grown alone at T2 (Analysis II) (Fig. 4a and b), iii) EHEC proteins overexpressed in co-culture at T2 compared with the expression level in co-culture at T1 (Analysis III) (Fig. 5a and b).

The 11 proteins proved to be differentially repressed in EHEC during the Analysis I were represented by 11 nodes (Figure 3a). Of these, 5 did not present interactions between them, while 2 groups of 3 proteins each were observed, mainly related to the metabolism and transport of amino acids. This also support the fact that E category resulted one of the most enriched in the hypergeometric analysis. Each group presented two interactions between their proteins. The proteins of the network are repressed proteins and had a fold change of 2.5 to 1.7. The network (Fig. 3b) shows the fold change of expression in absolute values and therefore demonstrates those proteins that presented greater repression. It is evident that the substrate binding protein

of the ABC transporter of arginine (ArtJ), 5-methyltetrahydropteroyl triglutamate-homocysteine methyltransferase (MetE) and large subunit 3-isopropyl malate dehydratase (LeuC) were those that were most repressed (2.5, 2.4 and 2.3 fold change respectively).

On the other hand, 19 proteins were repressed by EHEC in co-culture with respect to their individual growth at T2 and were represented in 16 nodes in Fig. 4a, since the identification of three of the spots resulted in the same protein (glutamate decarboxylase). In this network, three proteins did not interact with the rest and two proteins had an exclusive relationship between them. The interactions of greater magnitude were related to amino acid metabolism and transport, transcription and post-translational modifications (Fig. 4a). This group of EHEC proteins was repressed between 2.0 and 6.1 times in co-culture with respect to the individual culture of EHEC at T2. The periplasmic protein of binding to taurine (TauA) had the greatest repression (6.1 fold change), followed by alpha-ketoglutarate-dependent taurine dioxygenase protein (TauD) (4.5 fold change) (Fig. 4b). Because the overexpressed proteins (SucB and GlyA) in *E. coli* during co-culture at T2 were minority and belonging to different functional groups (energy production and conversion and amino acid metabolism, respectively) functional and interaction analysis was not carried out. It was focused on the majority repressed proteins at both analyzed time points (T1 and T2).

In the network observed in Fig. 5, the 13 proteins overexpressed during co-cultivation at T2 respect to T1 are represented, six of them did not present interaction with the rest. The most intense interactions were those involved in energy production and conversion and post-translational modifications. This set of proteins were overexpressed between 1.9 and 5.2 times by EHEC at T2 in co-culture, being TdcE (formate C-acetyltransferase) and ClpB (ATP-dependent chaperone) the proteins with greater expression difference (5.2 and 3.8 fold change respectively) both belonging to the most enriched categories according to the hypergeometric analysis (Fig. 5a and b; Fig. S2c; Table 2, Table S2).

3.2 Adhesion to extracellular matrix proteins: performance of EHEC during its coexistence with *Ent. mundtii* CRL35

In order to evaluate the ability to bind to ECM proteins, a microplate assay was applied using two proteins from ECM: collagen IV and laminin. The binding of EHEC and *Ent. mundtii* alone or in mixed suspensions was evaluated. Fig. 6 clearly shows that *Ent. mundtii* CRL35 has more than 80% adhesion

capacity for both ECM proteins (approximately 5 log CFU/mL adhered respect to 6 log CFU/mL seeded). In addition, enterococci adhesion was not modified when *E. coli* cells were present. The adhesion of *Ent. mundtii* CRL35 to laminin in the presence of *E. coli* NCTC12900 showed a slight increase although it is not statistically significant, as shown in Fig 6. On the other hand, EHEC, also demonstrated good binding capacity to both extracellular matrix proteins (about 70% of the added cells), just slightly lower than the binding observed for *Ent. mundtii* CRL35. However, EHEC adhesion capacity decreased when *Ent. mundtii* cells were present in the mixed cultures, reaching only 54% adhesion (3.14 - 3.23 log CFU/mL for collagen IV and laminin respectively) (Fig. 6). These findings suggest a competitive advantage of *Ent. mundtii* over EHEC on adhesion / colonization of food matrices during *Ent. mundtii*-EHEC interaction.

3.3 Potential activity of *Ent. mundtii* CRL35 as inducer of phage W933

The objective of this assay was to evaluate the possible induction of phage W933 by *Ent. mundtii* CRL35 during its interaction with *E. coli*. For this purpose, it was necessary to use a strain that bears the phage since *E. coli* NCTC12900 is a phage-free strain. Therefore, the strain *E. coli* C600Δtox was used as model for this assay, because it has lysogenic phage W933 in its genome. It is important to note that *stx* gene was replaced by the *gfp* gene (Green Fluorescent Protein). This strain allowed us to study the induction phenomenon without taking biosafety risks. The activation of the lytic cycle can be triggered by ciprofloxacin like other Shiga toxin-encoded by lysogenic bacteriophage (Zhang et al., 2000), which leads to the release of viral particles and the green fluorescence protein (GFP). The induction process after 4 and 24 h was monitored by cell count decrease during lysis (CFU/mL) and by viral particles counting (PFU/mL). Fig. 7 shows growth kinetics of C600Δtox under different treatments. In control conditions (with no induction), it presented an exponential growth during the first 6 h, reaching the stationary growth phase with 8.5 log CFU/mL, a level that remained fairly stable till the end of the incubation period. When *E. coli* lysis was induced with ciprofloxacin (positive control of induction), the performance of *E. coli* C600Δtox was modified with a sharp viability decrease after 3 h (approximately 3 log decrease). On the other hand, when *E. coli* C600Δtox growth was evaluated in the presence of *Ent. mundtii* CRL35, no change in viability was seen. In fact, the growth kinetics observed in this case resembled those observed in non-treated *E. coli* cells (Fig. 7). On the other hand, bacteriophage titers showed a significant increase only in samples treated with ciprofloxacin,

whereas a complete absence of PFU/ml was found when enterococci were present as occurred in non-treated samples (Table 3). These results suggest that the *Ent. mundtii* strain does not induce the lytic cycle of W933 phage. Overall, this finding indicates that the use of *Ent. mundtii* CRL35 as bioprotective strain to mitigate EHEC in meat would be a safe option.

4. Discussion

4.1 Differential protein expression assays

E. coli O157:H7 NCTC12900 was used as a model to carry out the proposed studies without compromising the biosafety because it is a natural mutant harboring virulence genes characteristic of the pathotype but it is not able to produce Shiga-type toxins (Dibb-Fuller et al., 2001). These features were validated in the present study (Table S3) and agree with those obtained by Ayaz, Gencay, & Erol (2014) who performed a molecular characterization of the main virulence and adhesion genes of different *E. coli* O157: H7 isolates from cattle in Turkey and used NCTC12900 strain as a control.

The present study focused on the interaction response of *E. coli* NCTC12900 during its co-culture with the bioprotective strain *Ent. mundtii* CRL35, which has inhibitory action towards this pathogen (Orihuel et al., 2018b). This LAB was selected for this study, due to its ability to inhibit *E. coli* O157:H7 and its well-known technological and bioprotective features (Orihuel et al., 2018a, 2018b; Saavedra, Minahk, de Ruiz Holgado, & Sesma, 2004; Salvucci, Saavedra, & Sesma, 2007). The growth kinetics of the studied strains were carried out using a meat based medium containing soluble compounds (proteins, vitamins, myoglobin among other meat constituents) that proved to be an optimal medium for LAB growth (Fadda et al. 1998, Orihuel et al. 2018a,b). In our previous study, we found that *Ent. mundtii* CRL 35 was among the LAB strains that produced the most significant reduction of EHEC viability during the co-culture in SMS. This strain triggered EHEC entrance into the death phase after 8 h of growth. Physiological results indicated that the inhibitory effect was not related to the LAB acidogenic potential nor to production of other soluble metabolites such as bacteriocins. In fact, *Ent. mundtii* presented a high inhibitory effect while displaying lower pH decrease than the other assayed LAB strains, thus indicating that the degree of inhibitory action was not related to the acidogenic potential. In addition, it was possible to corroborate the metabolic advantage of *Ent. mundtii* CRL35 during its coexistence with EHEC through its differential protein

expression. *Ent. mundtii,* during the co-culture, showed significant overexpression of proteins related mainly to carbohydrate / amino acid metabolisms, energy production, transcription/translation and cell division (Orihuel et al., 2018b). Herein, *E. coli* NCTC12900 evidenced strong down regulation of proteins belonging to different functional groups, at 6 and 30 h of growth in co-culture by comparison to its individual growth. The highest proportion of repressed proteins was related to amino acid metabolism at T1 and T2. Although other proteins such as those related to nucleotide metabolism at T1, and translation, protein folding and stress were also under-produced at 30 h (T2). This pattern reflects a low metabolic performance of this pathogen during the entrance into the death phase. In contrast, and as mentioned before, *Ent. mundtii* CRL35 was able to over express a wide range of proteins during the co-culture. Particularly, proteins related to carbohydrate metabolism such as phosphoglycerate kinase, fructose-bisphosphatealdolase, 6-phosphofructokinase, fructose-bisphosphatealdolase and enolase as well as some other involved in energy production and conversion such as pyruvate dehydrogenase E1 subunit alpha, L-lactate dehydrogenase, 2-oxoisovalerate dehydrogenase subunit beta, which clearly show a higher metabolic activity of *Ent. mundtii* (Orihuel et al. 2018b).

Even though there is scarce information regarding the differential expression of EHEC proteins in co-cultures with other microorganisms, the expression of EHEC proteins in response to different stressful conditions was widely studied. In this sense, (Bae, Yoon, Kim, & Lee, 2018) performed a comparative proteomic analysis of *E. coli* O157: H7 in order to investigate the effects of salt addition to acid treatment for pathogen reduction. In contrast to what was expected, differentially expressed proteins were not stress-related, but instead, they were mostly associated to energy metabolism. Interestingly, bacteria are able to develop resistance to several environmental stimuli when they are challenged with some particular stress factors, which is known as "cross tolerance". Exposure to such environmental stress agents induces the expression of proteins known as "stress/shock proteins", whose main function is to repair the damage caused by stress or eliminate the stressor agent (Yousef & Courtney, 2003). The master regulator of the general stress response in *E. coli* consists of a sigma subunit of the RNA polymerase, the RpoS factor (σS), which controls the expression of more than 35 genes involved in the response to stress (Bae et al., 2018). In our study, EHEC stress proteins were not the most affected, which would indicate that the pathogen was unable to trigger its complex system of resistance and tolerance against unfavorable conditions such as when *Ent.*

mundtii CRL35 is present in the meat medium. On the contrary, repression of a number of proteins involved in different metabolic pathways was observed. In this sense, Bi, Wang, Hu, and Liao (2017) who studied the molecular bases involved in the survival of sub-lethally injured *E. coli* O157: H7 cells (SIC) subjected to high pressure carbon dioxide (HPCD), showed that SIC survived treatment with HPCD by reducing carbohydrate hydrolysis, lipid / amino acid transport and metabolism, transcription and translation, DNA replication and repair. Thus, they proposed the formation of SIC with low metabolic activity as a survival strategy of *E. coli* O157: H7 against HPCD. In line with this, the general down regulation of protein expression observed herein in *E. coli* NCTC12900 could also be seen as an attempt of EHEC to survive in the hostile scenario dominated by *Ent. mundtii*. Nevertheless, death of EHEC was accelerated by the presence of *Ent. mundtii* CRL35 (Orihuel et al., 2018b). In fact, the pathogen grew exponentially until 8 h; thereafter, it entered unavoidably into the death phase. However, it is necessary to take into account the possible recovery of the remaining cells that were sub-lethally injured. In fact, Garcia-Gonzalez et al. (2007) postulated that SIC generated during treatment with HPCD could recover during storage under favorable conditions, which represents a potential risk to health hazard. That is why the idea of implementing a combination of additional barriers against the pathogen, that will avoid the recovery of sub-lethally injured cells, becomes important. This approach was described by Leistner (1994) and termed "hurdle technology", with each barrier being a moderate treatment that as a whole achieves a higher antimicrobial effectiveness with minimal loss of global quality of the food product. On the other hand, Kocharunchitt, King, Gobius, Bowman, and Ross (2012) carried out an interesting integrated transcriptomic and proteomic analysis to determine the physiological response of the *E. coli* O157: H7 strain Sakai to conditions of low temperature and low water activity that takes place during bovine carcasses cooling. The transcriptomic analysis revealed the activation of the master regulator of the stress response RpoS. In contrast, proteomic data revealed that several processes involved in protein synthesis were repressed, suggesting that *E. coli* can transcribe the required mRNA but may lack the cellular resources necessary for translation. Our findings are in line with such report and revealed a general repression of EHEC proteins during the co-culture with *Ent. mundtii* CRL35. These results could be explained by deficiencies in the protein translation system, which does not necessarily imply a decrease in the transcription of the genes involved.

When the comparative analysis was done between the two growth stages under co-culture conditions, EHEC showed overexpression of proteins during the death phase (T2). The proteins produced in higher amounts were related to amino acids / carbohydrates metabolism and stress. This possibly reflects a kind of futile struggle for surviving. However, for the same comparative analysis, Orihuel et al. (2018b) reported that *Ent. mundtii* CRL35 displayed overexpression of proteins during the first hours of co-culture (6 h). They are mostly involved in sugar and nitrogen metabolisms, which allowed high-energy production and optimal growth, establishing the competitive advantage over EHEC.

The present work highlights a repressed proteomic response of EHEC during the interaction with *Ent mundtii*, which confirms the metabolic disadvantage observed previously in the physiological approach (Orihuel et al., 2018b). In this vulnerability state, it could be expected that applying additional barriers to control EHEC will contribute to eliminate this pathogenic agent from meat. These results contribute to expand the knowledge on EHEC-*Ent mundtii* interaction and evidence that a number of mechanisms are involved in this interaction. Additional studies are necessary to explain how *Ent. mundtii* CRL35 antagonize effectively towards EHEC, at a molecular level. Therefore, the information collected through this proteomic approach helps to elucidate the global adaptive response of *E. coli* O157: H7 in a meat environment to allow the selection and / or development of effective strategies to fight this pathogen.

4.2 Adhesion to ECM components

Fibrous proteins are the predominant components of bovine ECM, comprising essentially collagen I, III and IV, insoluble fibronectin (i-fibronectin), laminin-a2 and elastin (Chagnot et al., 2013), all of which act as docking molecules for the adhesion of microorganisms to meat. Therefore, it is of high importance to know the capacity of pathogens and possible protective bacteria to bind key components of the ECM. Furthermore, it is crucial to know the reciprocal influence between these two groups of bacteria in the process of adhering to ECM proteins. Previous studies have shown that bacterial species such as *Salmonella* and *E. coli* O157: H7 preferentially adhere to connective tissue components, such as collagen fibers (Frank, 2001). In fact, our studies confirmed the ability of *E. coli* O157:H7 NCTC12900 to adhere to collagen IV and laminin. However, it could also be observed that the presence of *Ent. mundtii* CRL35 reduced the *E. coli* binding capacity to ECM proteins. Jin, Marquardt, and Zhao (2000) described a similar effect when using the *Ent.*

faecium 18C23, which effectively inhibited the adhesion of *E. coli* K88ac and K88MB to the intestinal mucus of pigs. The role of *Ent. mundtii* CRL35 on the adhesion capacity of EHEC is very important if we consider that the stronger the adhesion of microorganisms to meat surfaces, the harsher the physical and chemical processes needed for the complete elimination of them (Benedict, Schultz, & Jones, 1990; Fratamico, Schultz, Benedict, Buchanan, & Cooke, 1996; Tamblyn & Conner, 1997). On the other hand, *Ent. mundtii* CRL35 demonstrated optimal binding capacity to collagen IV and laminin. Previous studies indicate that AceA protein mediates the binding of *Ent. faecalis* OG1RF to type IV collagen, type I and laminin (Nallapareddy, Qin, Weinstock, Höök, & Murray, 2000). The obtained results indicate that *Ent. mundtii* CRL35 develops an effective competition strategy against the pathogen, having a specific advantage during the coexistence with EHEC on ECM proteins' adhesion. Supporting this idea, it should be noted that *Ent. mundtii* CRL35 overexpressed enolase, a moonlighting protein, during its coexistence with EHEC (Orihuel et al., 2018b). Enolase was described by Peng et al. (2014) as an actin binding protein in *Ent. faecalis*, which would indicate an additional competition strategy during meat adhesion. This information reflects the importance of understanding the process of bacterial binding to food matrixes, for the development of interventions that disturb pathogen colonization, which in turn will increase the effectiveness of decontamination.

4.3 Induction of the *E. coli* phage W933 by *Ent. mundtii* CRL35

As stated previously stated, the presence of *Ent. mundtii* CRL35 in SMS exerted an inhibitory effect on EHEC that is in turn reflected in a significant viability decrease of approx. 1.37 log CFU/mL in respect to the initial inoculum (Orihuel et al. 2018b). However, it was imperative to know whether the inhibition exerted by *Ent. mundtii* CRL35 was accompanied by the induction of the lytic cycle of the bacteriophage W933, which encodes the Stx1. In the case of Shiga toxin, it would be induced by the bioprotective strain and therefore food contamination with the toxin can be expected. This fact might definitely have a negative impact on the food safety and the use of *Ent. mundtii* CRL35 as bioprotective culture would therefore not be recommended. Nonetheless, our results indicated that *Ent. mundtii* CRL35 did not induce a decrease in the viability of *E. coli* C600Δtox nor induce lysis, thus indicating the bioprotective *Ent. mundtii* does not induce the lytic cycle of W933 phage present in C600. Thus, no expression and release of the Shiga toxin or viral

particles took place by action of *Ent. mundtii* CRL35. These findings are of great importance if we consider that Shiga toxin can be produced by EHEC in food (Rangel et al., 2005). Even sometimes the toxin was found only responsible for outbreaks of HUS, without the pathogen being present in the food (Goh et al., 2002). Supporting this idea, Rasooly and Do (2010) demonstrated that the Shiga 2 toxin is heat stable and that pasteurization of milk would not reduce the biological activity of Stx2. Furthermore, Robinson, Sinclair, Smith, and O'Brien (2006) found that Stx not only harms the host through its binding to globotriaosyl ceramide (Gb3) receptors with the subsequent protein synthesis inhibition, but also is able to increase the ability of EHEC to adhere to epithelial cells and colonize the intestine in mice. This effect would be produced by stimulation of the expression of nucleolin on the cell surface, an eukaryotic receptor for intimin (the main EHEC adhesin). This aspect further aggravates the presence of the toxin in food. Although this phenomenon requires more exhaustive studies, the obtained results predict the safe use of *Ent. mundtii* CRL35 as a bioprotective tool against EHEC, without contributing to the production of Stx in the food matrix.

5. Conclusion

The information collected through this study contributes to elucidate the response of *E. coli* O157: H7 during its interaction with a bioprotective LAB in a meat environment. Proteomic analysis showed a significant under expression of *E. coli* NCTC12900 proteins related to amino acid and nucleotide metabolisms in co-culture respect to its individual growth. On the other hand, the over expression of proteins mainly involved in stress, energy production, transcription and amino acid metabolism was achieved by EHEC during the co-culture at 30 h respect to 6 h. These proteomic results are in accordance with the physiological behavior previously observed. Therefore, the information collected through this proteomic approach elucidates the global adaptive response of *E. coli* O157: H7 in a meat environment to allow the selection and / or development of potential effective strategies to fight this pathogen. In addition, the disturbing effect of *Ent. muntii* on EHEC adhesion to EMC proteins during its co-existence is quite remarkable. These results indicate that *Ent. mundtii* CRL35 develops an effective competition strategy against the pathogen. Although Stx induction by LAB requires more exhaustive studies, the obtained results suggest the safe use of *Ent. mundtii* CRL35 as a bioprotective agent against EHEC, without inducing the

release of Stx to the food matrix. This work expands the knowledge on EHEC-*Ent mundtii* interaction and lays the basis for further studies to explain more specific mechanisms by which *Ent. mundtii* CRL35 antagonize effectively towards EHEC.

Acknowledgments

The mass spectrometry proteomics data have been deposited to the ProteomeXchange Consortium via the PRIDE (Perez-Riverol et al., 2019) partner repository with the dataset identifier PXD014588.

This work was financially supported by the research project from CONICET (PIP 0406; PIP 0530) and FONCyT Préstamo BID PICT 2011-0175 from Argentina. We thank CONICET for the doctoral scholarship of AO to support the completion of her doctoral degree.

Conflict of interests

Authors declare no conflict of interest.

References

Altschul, S. F, Gish, W., Miller, W., Myers, E.W. & Lipman, D. J. (1990). Basic local alignment search tool. *Journal of Molecular Biology, 215*(3), 403-10. https://doi.org/10.1016/S0022-2836(05)80360-2.

Ayaz, N. D, Gencay, Y. E. & Erol, I. (2014). Prevalence and molecular characterization of sorbitol fermenting and non-fermenting *Escherichia coli* O157: H7+/H7–isolated from cattle at slaughterhouse and slaughterhouse wastewater. *International Journal of Food Microbiology, 174*, 31-38. https://doi.org/0.1016/j.ijfoodmicro.2014.01.002.

Bae, Y. M., Yoon, J. H., Kim, J. Y. & Lee, S. Y. (2018). Identifying the mechanism of *Escherichia coli* O157: H7 survival by the addition of salt in the treatment with organic acids. *Journal of Applied Microbiology, 124*(1), 241-253. https://doi.org/10.1111/jam.13613.

Benedict, R., Schultz, F. & Jones, S. (1990). Attachment and removal of *Salmonella* spp. on meat and poultry tissues. *Journal of Food Safety, 11*(2),135-148. https://doi.org/10.1111/j.1745-4565.1990.tb00046.x,

Best, A., La Ragione, R. M., Cooley, W. A., O'Connor, C. D., Velge, P. & Woodward, M. J. (2003). Interaction with avian cells and colonisation of specific pathogen free chicks by Shiga-toxin negative *Escherichia coli* O157:H7 (NCTC12900). *Veterinary Microbiology, 93*(3), 207-22. https://doi.org/10.1016/S0378-1135(03)00031-2.

Bi, X., Wang, Y., Hu, X. & Liao, X. (2017). iTRAQ-Based Proteomic Analysis of Sublethally Injured *Escherichia coli* O157: H7 Cells Induced by High Pressure Carbon Dioxide. *Frontiers in Microbiology, 8*, 2544. https://doi.org/10.3389/fmicb.2017.02544.

Bonacina, J., Saavedra, L., Suárez, N. E., & Sesma, F. (2014). Draft genome sequence of the nonstarter bacteriocin-producing strain *Enterococcus mundtii* CRL35. *Genome Announc*., 2(3), e00444-14. https:// DOI: 10.1128/genomeA.00444-14.

Bustos, A. Y., de Valdez, G. F., Raya, R., de Almeida, A. M., Fadda, S. & Taranto, M. P. (2015). Proteomic analysis of the probiotic *Lactobacillus reuteri* CRL1098 reveals novel tolerance biomarkers to bile acid-induced stress. *Food Research International, 77*, 599-607. https://doi.org/10.1016/j.foodres.2015.10.001.

Candiano, G., Bruschi, M., Musante, L., Santucci, L., Ghiggeri, G.M., Carnemolla, B., Orecchia, P., Zardi, L. & Righetti, P.G. (2004). Blue silver: a very sensitive colloidal Coomassie G- 250 staining for proteome analysis. *Electrophoresis* 25, 1327-1333. https://doi.org/10.1002/elps.200305844.

Chagnot, C., Agus, A., Renier, S., Peyrin, F., Talon, R., Astruc, T. & Desvaux, M. (2013). *In vitro* colonization of the muscle extracellular matrix components by *Escherichia coli* O157: H7: the influence of growth medium, temperature and pH on initial adhesion and induction of biofilm formation by collagens I and III. *PLoS One*, 8(3), e59386. https://doi.org/10.1371/journal.pone.0059386.

Chagnot, C., Venien, A., Renier, S., Caccia, N., Talon, R., Astruc, T. & Desvaux, M. (2017). Colonisation of Meat by *Escherichia coli* O157: H7: Investigating Bacterial Tropism with Respect to the Different Types of Skeletal Muscles, Subtypes of Myofibres, and Postmortem Time. *Frontiers in Microbiology, 8*, 1366. https://doi.org/10.3389/fmicb.2017.01366.

Chen, J., Rossman, M. L. & Pawar, D. M. (2007). Attachment of enterohemorrhagic *Escherichia coli* to the surface of beef and a culture medium. *LWT-Food Science and Technology, 40*(2), 249-254. https://doi.org/10.1016/j.lwt.2005.10.011.

Daegelen, P., Studier, F. W., Lenski, R. E., Cure, S. & Kim, J. F. (2009). Tracing ancestors and relatives of *Escherichia coli* B, and the derivation of B strains REL606 and BL21 (DE3). *Journal of Molecular Biology, 394*(4), 634-643. https://doi.org/10.1016/j.jmb.2009.09.022.

Dibb-Fuller, M. P., Best, A., Stagg, D. A., Cooley, W. A., & Woodward, M. J. (2001). An in-vitro model for studying the interaction of *Escherichia coli* O157: H7 and other enteropathogens with bovine primary cell cultures. *Journal of Medical Microbiology*, 50(9), 759-769. https:// doi: 10.1099/0022-1317-50-9-759.

Fadda, S., Vignolo, G., Holgado, A. P. & Oliver, G. (1998). Proteolytic activity of *Lactobacillus* strains isolated from dryfermented sausages on muscle sarcoplasmic proteins. *Meat Science, 49*(1), 11-18. https://doi.org/10.1016/S0309-1740(97)00097-1.

Frank, J. F. (2001). Microbial attachment to food and food contact surfaces. *Advances in Food and Nutrition Research, 43*, 319-370. https://doi.org/10.1016/S1043-4526(01)43008-7.

Fratamico, P. M., Schultz, F. J., Benedict, R. C., Buchanan, R. L. & Cooke, P. H. (1996). Factors influencing attachment of *Escherichia coli* O157: H7 to beef tissues and removal using selected sanitizing rinses. *Journal of Food Protection, 59*(5), 453-459. https://doi.org/10.4315/0362-028X-59.5.453.

Galperin, M. Y., Makarova, K. S, Wolf, Y. I. & Koonin, E. V. (2015). Expanded microbial genome coverage and improved protein family annotation in the COG database. *Nucleic Acids Research, 43*,(Database issue):D261-9. https://doi.org/10.1093/nar/gku1223.

Gamage, S. D., Strasser, J. E., Chalk, C. L. & Weiss, A. A. (2003). Nonpathogenic *Escherichia coli* can contribute to the production of Shiga toxin. *Infection and Immunity, 71*(6), 3107-3115. https://doi.org/10.1128/IAI.71.6.3107-3115.2003.

Garcia-Gonzalez, L., Geeraerd, A. H, Spilimbergo, S., Elst, K., Van Ginneken, L., Debevere, J., Van Impe, J. & Devlieghere, F. (2007). High pressure carbon dioxide inactivation of microorganisms in foods: the past, the present and the future. *International Journal of Food Microbiology, 117*(1), 1-28. https://doi.org/10.1016/j.ijfoodmicro.2007.02.018.

Giaouris, E. (2015). Ability of foodborne bacterial pathogens to attach to meat and meat contact surfaces. *Biofilms in the Food Environment*, 145-175. https://doi.org/10.1002/9781118864036.ch6.

Goh, S., Newman, C., Knowles, M., Bolton, F., Hollyoak, V., Richards, S., Daley, P., Counter, D., Smith, H. & Keppie, N. (2002). *E. coli* O157 phage type 21/28 outbreak in North Cumbria associated with pasteurized milk. *Epidemiology & Infection 129*(3), 451-457. https://doi.org/10.1017/S0950268802007835.

Hussein, H. S. & Bollinger, L. M. (2005). Prevalence of Shiga toxin-producing *Escherichia coli* in beef. *Meat science, 71*(4), 676-89. https://doi.org/10.1016/j.meatsci.2005.05.012.

Jin, L., Marquardt, R. & Zhao, X. (2000). A strain of *Enterococcus faecium* (18C23) inhibits adhesion of enterotoxigenic *Escherichia coli* K88 to porcine small intestine mucus. *Applied and Environmental Microbiology, 66*(10),4200-4204. https://doi.org/10.1128/AEM.66.10.4200-4204.2000.

Johansen, B. K, Wasteson, Y., Granum, P. E. & Brynestad, S. (2001). Mosaic structure of Shiga-toxin-2-encoding phages isolated from *Escherichia coli* O157: H7 indicates frequent gene exchange between lambdoid phage genomes. *Microbiology, 147*(7), 1929-1936. https://doi.org/10.1099/00221287-147-7-1929.

Kocharunchitt, C., King, T., Gobius, K., Bowman, J. P. & Ross, T. (2012). Integrated transcriptomic and proteomic analysis of the physiological response of *Escherichia coli* O157: H7 Sakai to steady-state conditions of cold and water activity stress. *Molecular & Cellular Proteomics, 11*(1), M111. 009019. https://doi.org/10.1074/mcp.M111.009019

Leistner, L. (1994). Food design by hurdle technology and HACCP. Adalbert-Raps-Foundation. https://doi.org/10.1074/mcp.M111.009019.

Nallapareddy, S. R., Qin, X., Weinstock, G. M., Höök, M. & Murray, B. E. (2000). *Enterococcus faecalis* adhesin, ace, mediates attachment to extracellular matrix proteins collagen type IV and laminin as well as collagen type I. *Infection and Immunity, 68*(9), 5218-5224. https:// **doi:** 10.1128/IAI.68.9.5218-5224.2000

Nally, J. E., Grassmann, A. A., Planchon, S., Sergeant, K., Renaut, J., Seshu, J., McBride, A. J. & Caimano, M. J. (2017). Pathogenic leptospires modulate protein expression and post-translational

modifications in response to mammalian host signals. *Frontiers in Cellular and Infection Microbiology*, 7, 362. https://doi.org/10.3389/fcimb.2017.00362.

O'Brien, A. D., Newland, J. W., Miller, S. F., Holmes, R. K., Smith, H. W. & Formal, S. B. (1984). Shiga-like toxin-converting phages from *Escherichia coli* strains that cause hemorrhagic colitis or infantile diarrhea. *Science, 226*(4675), 694-696. https://doi.org/10.1016/0882-4010(89)90080-6.

Orihuel, A., Bonacina, J., Vildoza, M. J, Bru, E., Vignolo, G., Saavedra, L. & Fadda, S. (2018a). Biocontrol of *Listeria monocytogenes* in a meat model using a combination of a bacteriocinogenic strain with curing additives. *Food Research International,* 107, 289-296. https://doi.org/10.1016/j.foodres.2018.02.043.

Orihuel, A., Terán, L., Renaut, J., Vignolo, G. M., De Almeida, A. M., Saavedra, M. L. & Fadda, S. (2018b). Differential Proteomic Analysis of Lactic Acid Bacteria—*Escherichia coli* O157: H7 Interaction and Its Contribution to Bioprotection Strategies in Meat. *Frontiers in Microbiology, 9*. https://doi.org/10.3389/fmicb.2018.01083.

Peng, Z., Krey, V., Wei, H., Tan, Q., Vogelmann, R., Ehrmann, M. A. & Vogel, R. F. (2014). Impact of actin on adhesion and translocation of *Enterococcus faecalis*. *Archives of Microbiology, 196*(2), 109-117. https://doi.org/10.1007/s00203-013-0943-1.

Perez-Riverol, Y., Csordas, A., Bai, J., Bernal-Llinares, M., Hewapathirana, S., Kundu, D.J, Inuganti, A., Griss, J., Mayer, G., Eisenacher, M., Pérez, E., Uszkoreit, J., Pfeuffer, J., Sachsenberg, T., Yilmaz, S., Tiwary, S., Cox, J., Audain, E., Walzer, M., Jarnuczak, A.F., Ternent, T., Brazma, A., Vizcaíno, J.A. (2019). The PRIDE database and related tools and resources in 2019: improving support for quantification data. *Nucleic Acids Research,* 47(D1), 442-450 (PubMed ID: 30395289).

Rangel, J. M., Sparling, P. H., Crowe, C., Griffin, P. M. & Swerdlow, D. L. (2005). Epidemiology of *Escherichia coli* O157: H7 outbreaks, united states, 1982–2002. *Emerging Infectious Diseases, 11*(4),603. https://doi.org/10.3201/eid1104.040739.

Rasooly, R. & Do, P. M. (2010). Shiga toxin Stx2 is heat-stable and not inactivated by pasteurization. *International Journal of Food Microbiology, 136*(3), 290-294. https://doi.org/10.1016/j.ijfoodmicro.2009.10.005.

Rivas, L., Dykes, G. A. & Fegan, N. (2006). Attachment of Shiga toxigenic *Escherichia coli* to beef muscle and adipose tissue. *Journal of Food Protection, 69*(5), 999-1006. https://doi.org/10.4315/0362-028X-69.5.999.

Robinson, C. M, Sinclair, J. F, Smith, M. J. & O'Brien, A. D. (2006). Shiga toxin of enterohemorrhagic *Escherichia coli* type O157: H7 promotes intestinal colonization. *Proceedings of the National Academy of Sciences 103*(25), 9667-9672. https://doi.org/10.1073/pnas.0602359103.

Saavedra, L., Minahk, C., de Ruiz Holgado, A.P. & Sesma, F. (2004). Enhancement of the enterocin CRL35 activity by a synthetic peptide derived from the NH2-terminal sequence. *Antimicrob Agents Chemother* 48(7)**,** 2778-2781. doi: 10.1128/AAC.48.7.2778-2781.2004.

Salvucci, E., Saavedra, L. & Sesma, F. (2007). Short peptides derived from the NH2-terminus of subclass IIa bacteriocin enterocin CRL35 show antimicrobial activity. *The Journal of Antimicrobial Chemotherapy* 59(6):1102-8. https://doi.org/10.1093/jac/dkm096.

Shannon, P., Markiel, A., Ozier, O., Baliga, N. S., Wang, J. T., Ramage, D., Amin, N., Schwikowski, B. & Ideker, T. (2003). Cytoscape: a software environment for integrated models of biomolecular interaction networks. *Genome Research, 13*(11), 2498-2504. https://doi.org/10.1101/gr.1239303.

Sperandio, V. & Pacheco, A.R. (2012). Shiga toxin in enterohemorrhagic *E. coli*: regulation and novel anti-virulence strategies. *Frontiers in Cellular and Infection Microbiology* 2:81. https://doi.org/10.3389/fcimb.2012.00081.

Szklarczyk, D., Franceschini, A., Wyder, S., Forslund, K., Heller, D., Huerta-Cepas, J., Simonovic, M., Roth, A., Santos, A., Tsafou, K. P., Kuhn, M., Bork, P., Jensen, L. J. & von Mering, C. (2015). STRING v10: protein-protein interaction networks, integrated over the tree of life. *Nucleic Acids Research 43*, (Database issue):D447-52. https://doi.org/10.1093/nar/gku1003.

Taboada B., Estrada K., Ciria R. & Merino E. (2018) Operon-mapper: a web server for precise operon identification in bacterial and archaeal genomes. *Bioinformatics*, 34(23), 4118–4120. https://doi: 10.1093/bioinformatics/bty496.

Tamblyn, K. C. & Conner, D. E. (1997). Bactericidal Activity of Organic Acids against *Salmonella typhimurium* Attached to Broiler Chicken Skint. *Journal of Food Protection, 60*(6), 629-633. https://doi.org/10.4315/0362-028X-60.6.629.

Walker, G. C. (1996). The SOS response of *Escherichia coli*. *Escherichia coli and Salmonella. Cellular and Molecular Biology*, 1400-1416

Weeratna, R. D. & Doyle, M. P. (1991). Detection and production of verotoxin 1 of *Escherichia coli* O157: H7 in food. *Applied and Environmental Microbiology, 57*(10), 2951-2955.

Yousef, A. E. & Courtney, P. D. (2003). Basics of stress adaptation and implications in new-generation foods. *Microbial Stress Adaptation and Food Safety, 1*, 1-30.

Zhang, X., McDaniel, A. D., Wolf, L. E., Keusch, G. T., Waldor & M. K., Acheson, D. W. (2000). Quinolone antibiotics induce Shiga toxin-encoding bacteriophages, toxin production, and death in mice. *The Journal of Infectious Diseases, 181*(2), 664-670. https://doi.org/10.1086/315239.

Figure 1. 2DE gels showing the proteome of *E. coli* NCTC12900. 2DE map of *E. coli* and *Ent. mundtii* proteomes shown for each analysis. The *E. coli* O157:H7 NCTC12900 differentially expressed proteins are shaded and numbered. Analysis I: *E. coli* NCTC12900 growing in co-culture with *Ent. mundtii* CRL35 versus *E. coli* growing individually at T1; Analysis II: *E coli* growing in co-culture versus *E. coli* growing individually at T2 and Analysis III: *E coli* growing in co-culture at T1 versus T2.

Figure 2. Pie chart illustrating the percentage distribution of proteins differentially expressed by *E. coli* O157:H7 NCTC12900 identified by their predicted functional categories. (a) Proteins repressed in co-culture at T1 versus individual culture at T1; (b) Proteins repressed in co-culture at T2 versus individual culture at T2; (c) Overexpressed proteins during co-culture at T2 versus T1.

Figure 3. Interaction network of proteins repressed in *E. coli* O157:H7 NCTC12900 in co-culture with respect to their individual culture at T1. Proteins are represented by nodes while their interactions by edges. The strength of the different interactions is given by the thickness of the edges. (a) Network built using STRING v10.05. Proteins related to the metabolism and transport of amino acids are grouped in the circle. (b) Network built using Cytoscape v3.6.1. The size of the nodes proportionally represents the fold change in absolute values of each represented protein. The range of colors presented in edges and nodes

indicate the magnitude of the interaction and fold change expression respectively, with the highest values represented in clear grey (pink) and the smaller ones in dark (violet).

IlvD: Dihydroxy-acid dehydratase, FusA: elongation factor G, NusA: Transcription termination /antitermination protein, CarA: carbamoyl-phosphate synthase small chain, LeuC: 3-isopropylmalate dehydratase large subunit, AckA: acetate kinase, MetB: cystathionine gamma-synthase, ArtJ: arginine ABC transporter periplasmic binding protein, MetE: methyltetrahydropteroyltri. glutamate--homocysteine S-methyltransferase, SlyD: FKBP-type peptidylprolyl cis-trans isomerase, GuaB: inosine 5'-.monophosphate dehydrogenase.

Figure 4. Interaction network of proteins repressed in *E. coli* O157:H7 NCTC12900 in co-culture with respect to their individual culture at T2. Proteins are represented by nodes while their interactions by edges. The strength of the different interactions is given by the thickness of the edges. (a) Network built using STRING v10.05. The groups of proteins indicated by circles are related to amino acid metabolism and transport, transcription and post-translational modifications. (b) Network built using Cytoscape v3.6.1. The size of the nodes proportionally represents the fold change in absolute values of each protein represented. The range of colors presented in edges and nodes indicate the magnitude of the interaction and fold change respectively, with the highest values represented in light grey (pink) and the smaller ones in dark (violet).

PheT: phenylalanine—tRNA ligase beta subunit, LeuS: leucine--tRNA ligase, GapA: glyceraldehyde-3-phosphate dehydrogenase A, GrpE: chaperone protein, DnaK: chaperone protein, OmpC: outer membrane Porin C, PepN: aminopeptidase N, GlnA: bifunctional glutamine synthetase adenylyl transferase /adenylyl removing enzyme, MetB: cystathionine gamma-synthase, TdcE: formate C-acetyltransferase, KatG1: catalase-peroxidase 1, GadB: glutamate decarboxylase, GadA: Glutamate decarboxylase, partial, EfeO: iron uptake system component, TauA: taurine ABC transporter periplasmic binding protein, TauD: taurine dioxygenase.

Figure 5. Interaction network of overexpressed proteins in co-culture at T2 with respect to co-culture at T1. Proteins are represented by nodes while their interactions by edges. The strength of the different interactions is given by the thickness of the lines. (a) Network built using STRING v10.05. The proteins

grouped by the circle are the ones related to the production and conversion of energy and post-translational modifications. (b) Network built using Cytoscape v3.6.1. The size of the nodes proportionally represents the fold change of each protein represented. The range of colors presented in edges and nodes indicate the magnitude of the interaction and fold change respectively, with the highest values represented in light grey (pink) and the smaller ones in dark (violet).

PyrG: CTP synthase, PurR: HTH.type transcriptional repressor, PtsI: phosphoenol pyruvate-protein phosphotransferase, Pta: phosphate acetyltransferase, TdcE: formate C-acetyltransferase, Mdh: malate dehydrogenase, GadB: glutamate decarboxylase beta, DapD: 2,3,4,5-tetrahydropyridine-2,6-dicarboxylate N-succinyltransferase, MdoG: Glucans biosynthesis protein, KatG: catalase-peroxidase 1, ArcA: aerobic respiration control protein, ClpB: Chaperone protein, HtpG: Chaperone protein.

Figure 6. Boxplots showing the adhesion capacity to collagen IV (a) and laminin (b) of *E. coli* O157:H7 NCTC12900 and *Ent. mundtii* CRL35 as individual or mixed cultures (EHEC- *Ent. mundtii*). The level of adhesion was expressed as log CFU/mL of adhered cells. Mean values are represented by the black squares. Different letters indicate significant differences according to theTukey test ($p < 0.05$).

Figure 7. Viability of *E. coli* C600Δtox (CFU/mL) in LB at 37 °C. Individual growth (black line), in the presence of Ciprofloxacin (ATB) (dotted line) and in the presence of *Ent. mundtii* CRL35 (grey line) are represented.

Table 1. Differentially expressed proteins by *E. coli* O157:H7 NCTC12900 during its growth in co-culture, respect to its individual growth at T1 and T2 in sarcoplasmic model system at 30 °C.

Function	COG[a]	Protein name and abbreviation	Spot #/UniProt entry[b]	MASCOT Score[c]	Coverage %[d]	# matching peptides[e]	MM / pI[f]	Fold Change[g]
T1: Exponential growth phase (6 h, co-culture /individual growth)								
Energy production and conversion	C	Acetate kinase **AckA**	**1**/P0A6A5	923	74	32	43619/ 5.85	-1.8
Transcription	K	Transcription termination /antitermination protein **NusA**	**2**/P0AFF8	1020	70	52	42261/ 4.53	-1.8

Amino acid metabolism	E	5-Methyltetrahydropteroyltri.glutamate--homocysteine S-methyltransferase **MetE**	**3**/ Q8L8X5	1220 1200 1210	52 45 43	57 49 47	85126/ 5.61	-2.4 -2.4 -2.1
	E	Cystathionine gamma-synthase **MetB**	**4**/Q8X768	1240	51	30	41825/ 6.13	-1.7
	E G	Dihydroxy-acid dehydratase **IlvD**	**5**/Q8XQAV1	1050	54	43	64617/ 5.59	-1.8
	E	3-isopropylmalate dehydratase large subunit **LeuC**	**6**/Q8XA00	916	53	32	50363/ 5.90	-2.3
	E T	Arginine ABC transporter periplasmic binding protein **ArtJ**	**7**/A0A0H3JDO3	756	69	29	27001 / 6.31	-2.5
Protein folding	O	FKBP-type peptidylprolyl cis-trans isomerase **SlyD**	**8**/P0A9L1	472	70	19	15265/ 4.31	-1.7
Translation	J	Elongation factor G **FusA**	**9**/P0A6N0	1220	70	53	77677 / 5.24	-1.7
Nucleotide metabolism	E F	Carbamoyl-phosphate synthase small chain **CarA**	**10**/P0A6F2	752	43	22	41653/ 5.91	-1.9
	F R	Inosine 5'-.monophosphate dehydrogenase **GuaB**	**11**/P0ADG8	1460	53	34	52303/ 6.02	-1.9
T2: death phase (30 h, co-culture / 96 h, individual culture)								
Carbohydrate metabolism	G	Glyceraldehyde-3-phosphate dehydrogenase A **GapA**	**12**/P0A9B4	744	72	29	31252/ 6.61	-2.0
Energy production and conversion	C	Formate C-acetyltransferase **TdcE**	**13**/Q8XEB4	1080	61	57	82365/ 5.69	-2.7
	C	Dihydrolipoyllysine-residue succinyltransferase component of 2-oxoglutarate dehydrogenase complex **SucB**	**14**/P0AFG7	947	55	36	43942/ 5.58	+2.0
Amino acid metabolism	E	Cystathionine gamma-synthase **MetB**	**15**/Q8X768	1080	52	27	48565/ 6.16	-2.5
	E	Glutamate decarboxylase, **GadA**	**16**/P58228	453	49	35	53120/ 5.22	-3.0
			17/P58228	537	41	21	53120/ 5.22	-2.9
			18/P58228	632	46	36	53120/ 5.22	-3.0

	E	Glutamate decarboxylase **GadB**	**19**/P69911	539	43	34	53264/ 5.29	-3.1
			20/P69911	483	45	35	53264/ 5.29	-2.4
	E	Bifunctional glutamine synthetase adenylyl transferase /adenylyl removing enzyme **GlnA**	**21**/Q8XBM3	861	63	33	52159/ 5.26	-2.4
	E	Serine hydroxymethyltransferase **GlyA**	**22**/Q8XA55	739	62	34	45477 / 6.03	+2.8
	E	Aminopeptidase N **PepN**	**23**/Q8XDE6	826	35	40	99371/ 5.12	-2.5
Translation	J	Leucine--tRNA ligase **LeuS**	**24**/Q8XBN8	895	47	58	97831/ 5.11	-2.4
	J R	Phenylalanine—tRNA ligase beta subunit **PheT**	**25**/Q8XE32	1150	52	60	88091/ 5.17	-2.1
Protein folding	O	Chaperone protein **DnaK**	**26**/P0A6Z0	1760	68	57	69216/ 4.83	-2.4
	O	Chaperone protein **GrpE**	**27**/Q7ABI1	490	61	16	16896/ 4.47	-3.1
Stress	P	Catalase-peroxidase 1 **KatG1**	**28**/Q7A978	1030	51	52	80031 / 5.14	-3.2
	P	Iron uptake system component **EfeO**	**29**/Q8XAS6	1120	83	40	39444/ 4.86	-2.1
Transport	P	Taurine ABC transporter periplasmic binding protein **TauA**	**30**/Q8X517	1240	62	28	31575/ 6.33	-6.1
	M	Outer membrane Porin C **OmpC**	**31**/Q8XE41	1030	64	30	40483 / 4.55	-2.3
Secondary metabolites catabolism	Q	Taurine dioxygenase **TauD**	**32**/Q8X512	1130	73	37	32350/ 6.27	-4.5

[a] Functional category according to COG database where each letter represents the different COG functional categories: G: carbohydrate metabolism and transport; C: energy production and conversion; K: transcription; Q: secondary metabolites biosynthesis; R: general functional prediction only; M: cell wall structure and biogenesis and outer membrane; E: amino acid transport and metabolism; O: molecular chaperones and related functions; J: translation, including ribosome structure and biogenesis; T: signal transduction mechanisms; F: nucleotide transport and metabolism and P: inorganic ion transport and metabolism

[b] Spot designations correspond to those of the gels shown in Figure 1 (Analysis I and II) /Accession code in the UniProt database.

[c] Protein Score is -10 *Log (P), where P is the probability that the observed match is a random event. Proteins scores larger than 81 are considered significant (P <0.05).

[d] % Mass coverage obtained by Peptide Mass Fingerprint search

[e] Number of peptide matches (from the Peptide Mass Fingerprint search)

[f] Molecular Mass (Da) / Calculated isoelectric point

[g] Relative Fold change: Normalized volumes of protein spot in co-culture / normalized volumes of protein spots in individual growth.

Table 2. Differentially expressed proteins by *E. coli* O157:H7 NCTC12900 during its growth in co-culture at T2 respect to the co-culture at T1 in a sarcoplasmic model system at 30 °C

Function	COG	Protein name and abbreviation	Spot#/UniProt entry[b]	MASCOT Score[c]	Coverage %[d]	# matching peptides[e]	MM /pI[f]	Fold change[g]
Carbohydrate metabolism	G	Phosphoenol pyruvate-protein phosphotransferase **PtsI**	**33**/Q8XBL3	166	42	18	63708/ 4.77	2.5
Energy production and conversion	C	Malate dehydrogenase **Mdh**	**34**/P61891	149	24	5	28317/ 5.61	2.1
	C	Formate C-acetyltransferase **TdcE**	**35**/Q8XEB4	236	29	28	82365/ 5.62	5.2
	R C	Phosphate acetyltransferase **Pta**	**36**/Q8XCU8	315	29	20	56200/ 5.39	2.3
Amino acid metabolism	E	Glutamate decarboxylase beta **GadB**	**37**/P69911	163	39	11	46850/ 5.25	2.6
	E	2,3,4,5-tetrahydropyridine-2,6-dicarboxylate N-succinyltransferase **DapD**	**38**/Q8X8Y7	171	37	11	30030/ 5.56	2.0
Nucleotide metabolism	F	CTP synthase **PyrG**	**39**/P0A7E7	192	22	12	56285/ 5.63	2.1
Transcription	K	HTH.type transcriptional repressor **PurR**	**40**/P0ACP8	79	37	5	16098/ 5.62	2.2
	T K	Aerobic respiration control protein **ArcA**	**41**/P0A9Q3	143	19	3	27349/ 5.14	2.5
Stress	O	Chaperone protein **ClpB**	**42**/P63285	160	23	21	95428/ 5.33	3.8
	O	Chaperone protein **HtpG**	**43**/P0A6Z5	116	8	4	65179/ 5.09	2.9
	P	Catalase-peroxidase 1 **KatG1**	**44**/Q7A978	199	18	13	80017/ 5.14	2.4
Cell wall biosynthesis	P	Glucans biosynthesis protein **MdoG**	**45**/P67556	141	26	13	58646/ 6.70	1.9

[a] Functional category according to COG database where each letter represents the different COG functional categories: G: carbohydrate metabolism and transport; C: energy production and conversion; K: transcription; Q: secondary metabolites biosynthesis; R: general functional prediction only; M: cell wall structure and biogenesis and outer membrane; E: amino acid transport and metabolism; O: molecular chaperones and related functions; J: translation,

including ribosome structure and biogenesis; F: Nucleotide transport and metabolism; P: Inorganic ion transport and metabolism and T: Signal transduction mechanisms

[b] Spot designations correspond to those of the gels shown in Figure 1 (Analysis III)/Accession code in the UniProt database.

[c] Protein Score is -10 *Log (P), where P is the probability that the observed match is a random event. Protein scores >75 are considered significant (P <0.05)

[d] % Mass coverage obtained by Peptide Mass Fingerprint search

[e] Number of peptide matches (from the Peptide Mass Fingerprint search)).

[f] Molecular Mass (Da)/ Calculated isoelectric point

[g] Relative Fold change: Normalized volumes of protein spot in co-culture T2/ normalized volumes of protein spots in co-culture T1.

Table 3. Titration of phage W933 present in the supernatant of *E. coli* C600Δtox culture (Log PFU/ml) when cultured alone (control), in the presence of the antibiotic (ciprofloxacin) or in the presence of *Ent. mundtii* CRL35, after 4 and 24 h at 30 ° C

Treatment/Time	**Control**	**Ciprofloxacin 60 ng/ml**	***Ent. mundtii* CRL35 (10^7 CFU/ml)**
T4	nd	6.7 Log PFU/ml	nd
T24	nd	7.0 Log PFU/ml	nd

nd: not detected

Graphical abstract:

Highlights

- *E. coli* O157:H7 (EHEC) proteome variations due to lactic acid bacteria (LAB) presence
- Proteomics support EHEC - LAB physiological behavior in meat
- Decreased EHEC adhesion occurred when LAB was co-inoculated with EHEC
- Absence of toxin induction by LAB strain suggests its safe use as bioprotector in meat
- A contribution to molecular mechanisms of EHEC-LAB interaction is provided

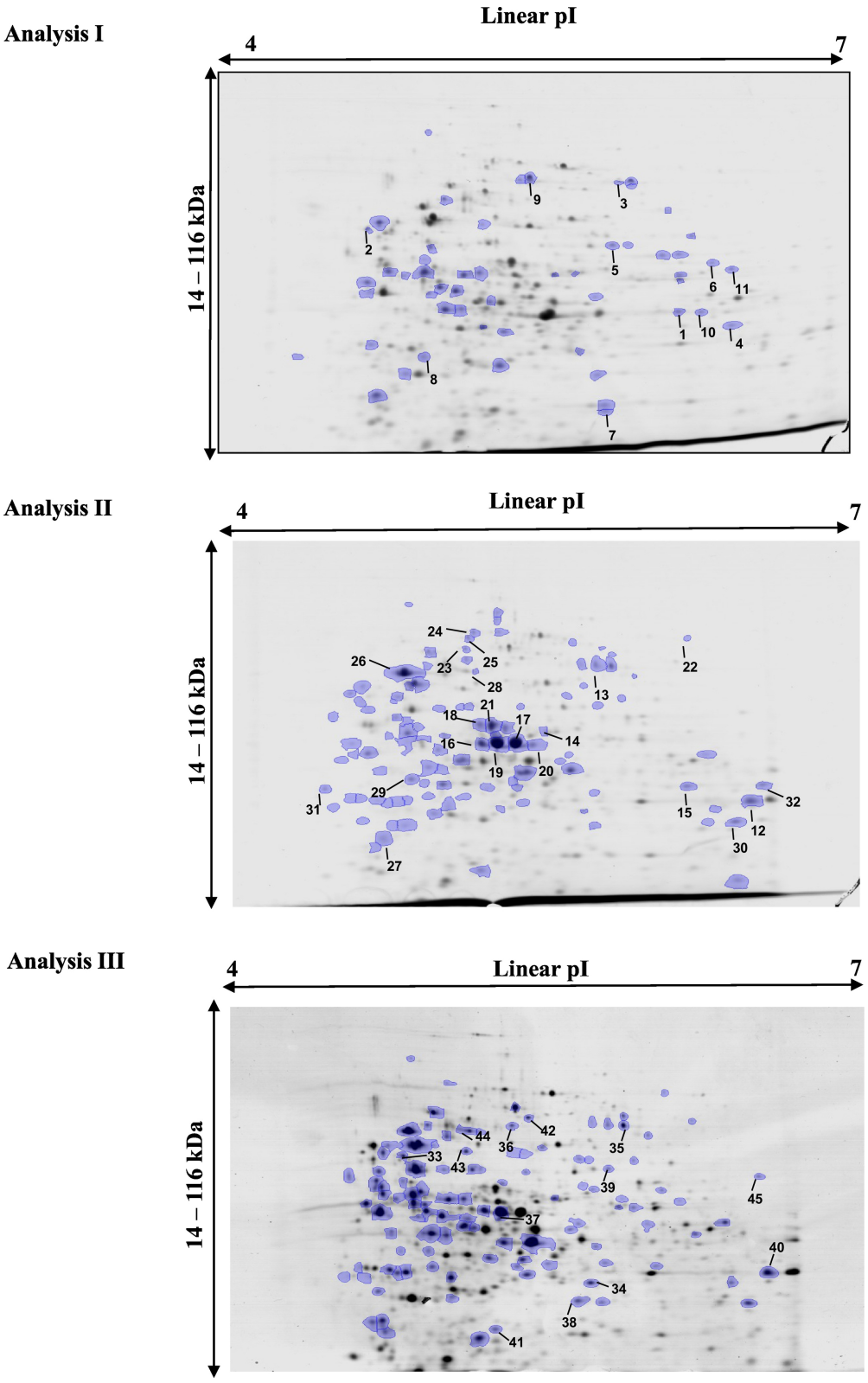
Analysis I
Linear pI
4
7
14 – 116 kDa
9
3
2
5
6
11
1
10
4
8
7
Analysis II
Linear pI
4
7
14 – 116 kDa
24
26
25
23
28
22
13
21
18
17
14
16
19
20
29
31
15
32
12
30
27
Analysis III
Linear pI
4
7
14 – 116 kDa
42
44
36
35
33
43
39
45
37
40
34
38
41

Figure 1

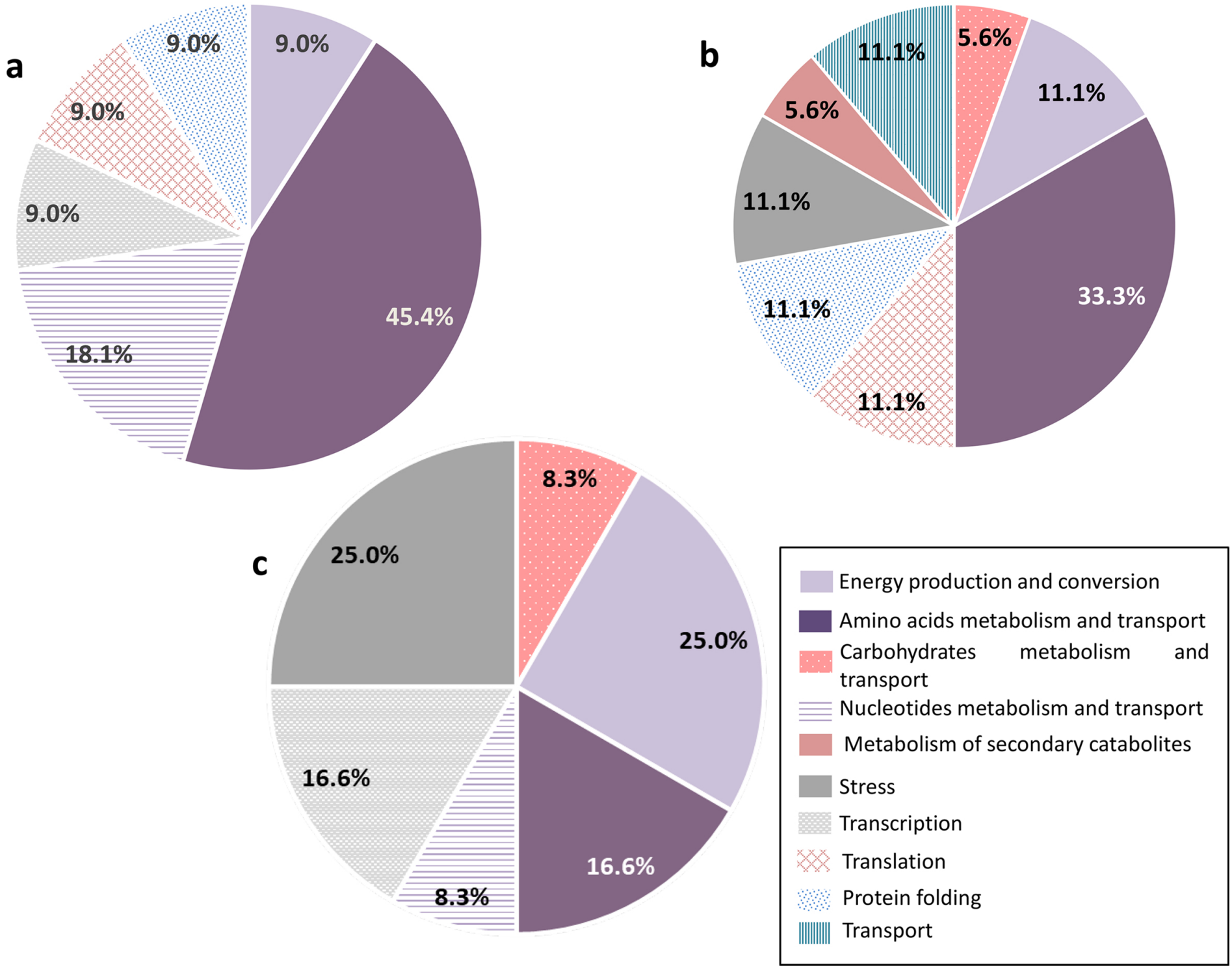
a
9.0%
9.0%
9.0%
9.0%
45.4%
18.1%
b
11.1%
5.6%
11.1%
5.6%
11.1%
11.1%
11.1%
33.3%
c
8.3%
25.0%
25.0%
16.6%
16.6%
8.3%
Energy production and conversion
Amino acids metabolism and transport
Carbohydrates metabolism and transport
Nucleotides metabolism and transport
Metabolism of secondary catabolites
Stress
Transcription
Translation
Protein folding
Transport

Figure 2

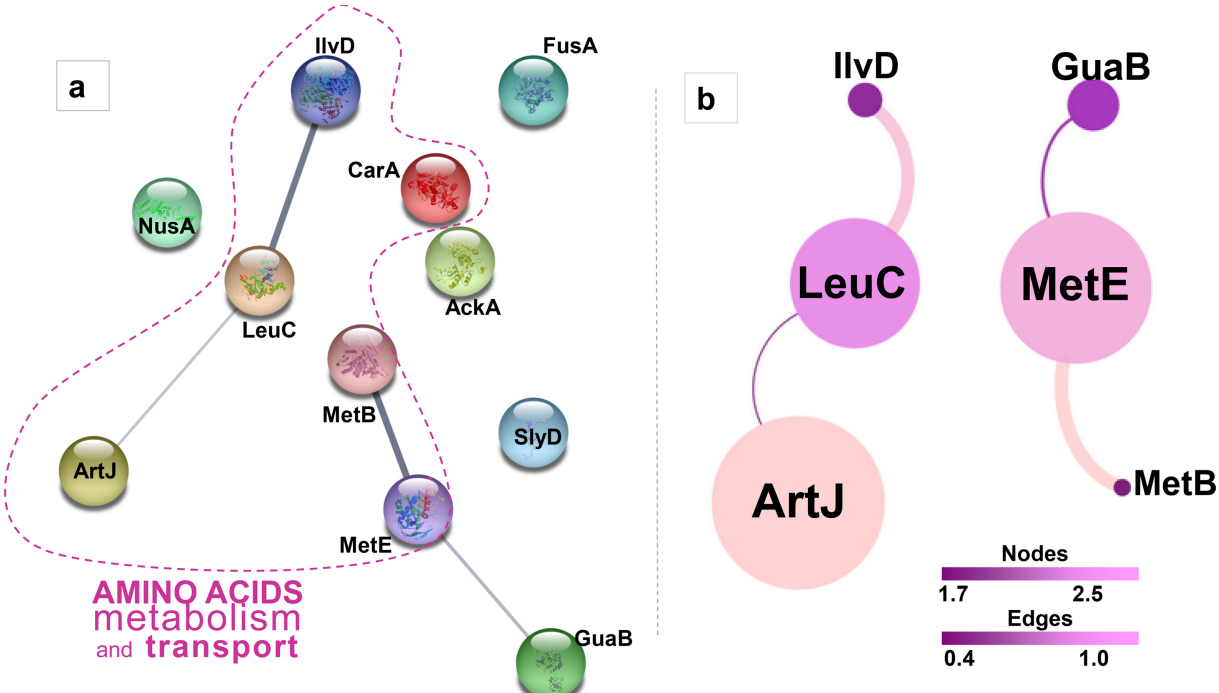
a
IlvD
FusA
CarA
NusA
AckA
LeuC
MetB
SlyD
ArtJ
MetE
GuaB
AMINO ACIDS
metabolism
and transport
b
IlvD
GuaB
LeuC
MetE
ArtJ
MetB
Nodes
1.7
2.5
Edges
0.4
1.0

Figure 3

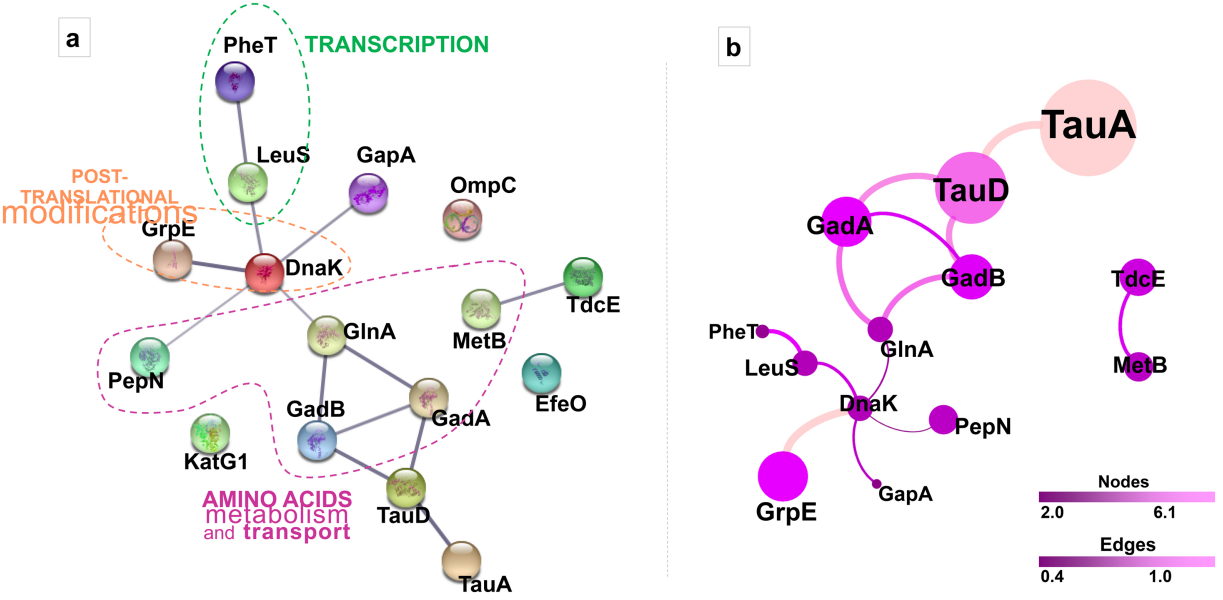
a
PheT
TRANSCRIPTION
LeuS
GapA
OmpC
POST-
TRANSLATIONAL
modifications
GrpE
DnaK
TdcE
MetB
GlnA
PepN
EfeO
GadB
GadA
KatG1
AMINO ACIDS
metabolism
and transport
TauD
TauA
b
TauA
TauD
GadA
GadB
TdcE
PheT
GlnA
MetB
LeuS
DnaK
PepN
GapA
GrpE
Nodes
2.0
6.1
Edges
0.4
1.0

Figure 4

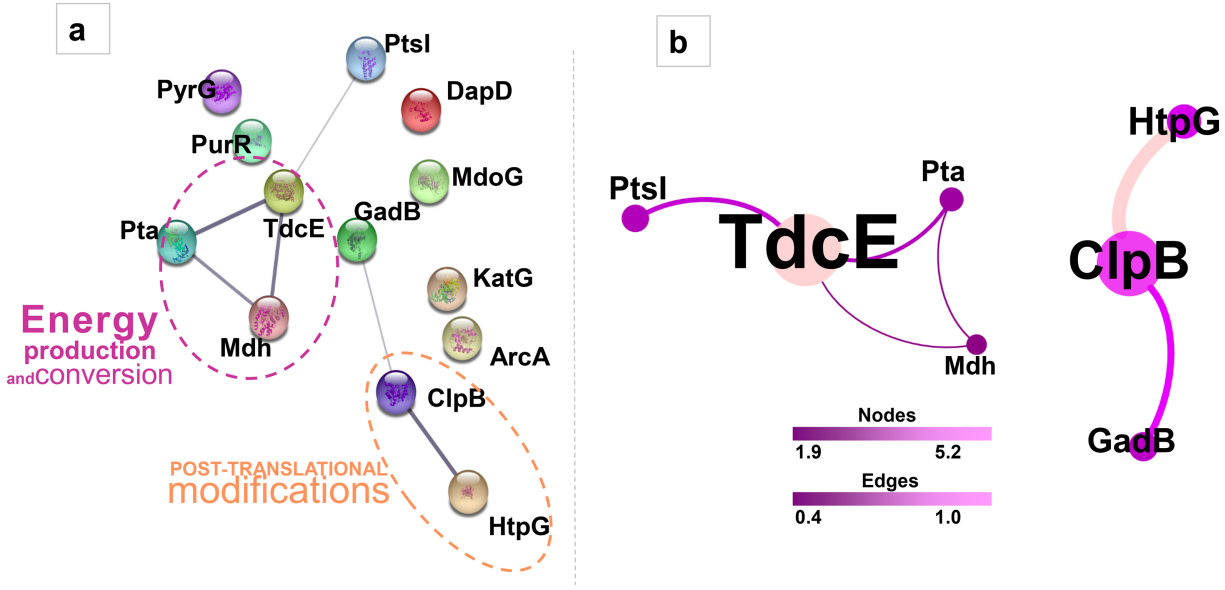
a
PtsI
PyrG
DapD
PurR
MdoG
Pta
TdcE
GadB
KatG
Energy
production
and conversion
Mdh
ArcA
ClpB
POST-TRANSLATIONAL
modifications
HtpG
b
PtsI
Pta
TdcE
Mdh
HtpG
ClpB
GadB
Nodes
1.9
5.2
Edges
0.4
1.0

Figure 5

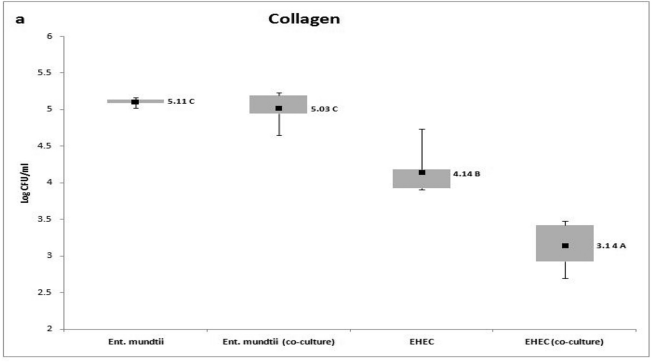
a
Collagen
log CFU/ml
6
5.5
5
4.5
4
3.5
3
2.5
2
5.11 C
5.03 C
4.14 B
3.14 A
Ent. mundtii
Ent. mundtii (co-culture)
EHEC
EHEC (co-culture)

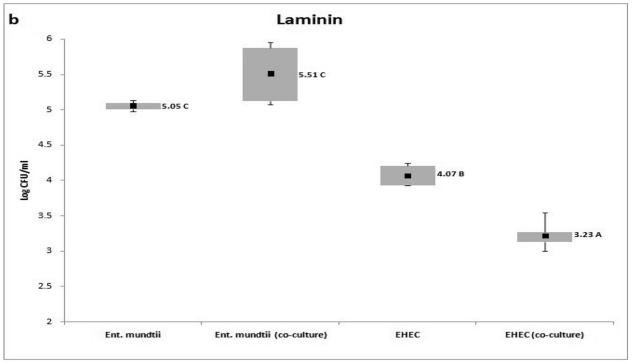
b
Laminin
log CFU/ml
6
5.5
5
4.5
4
3.5
3
2.5
2
5.05 C
5.51 C
4.07 B
3.23 A
Ent. mundtii
Ent. mundtii (co-culture)
EHEC
EHEC (co-culture)

Figure 6

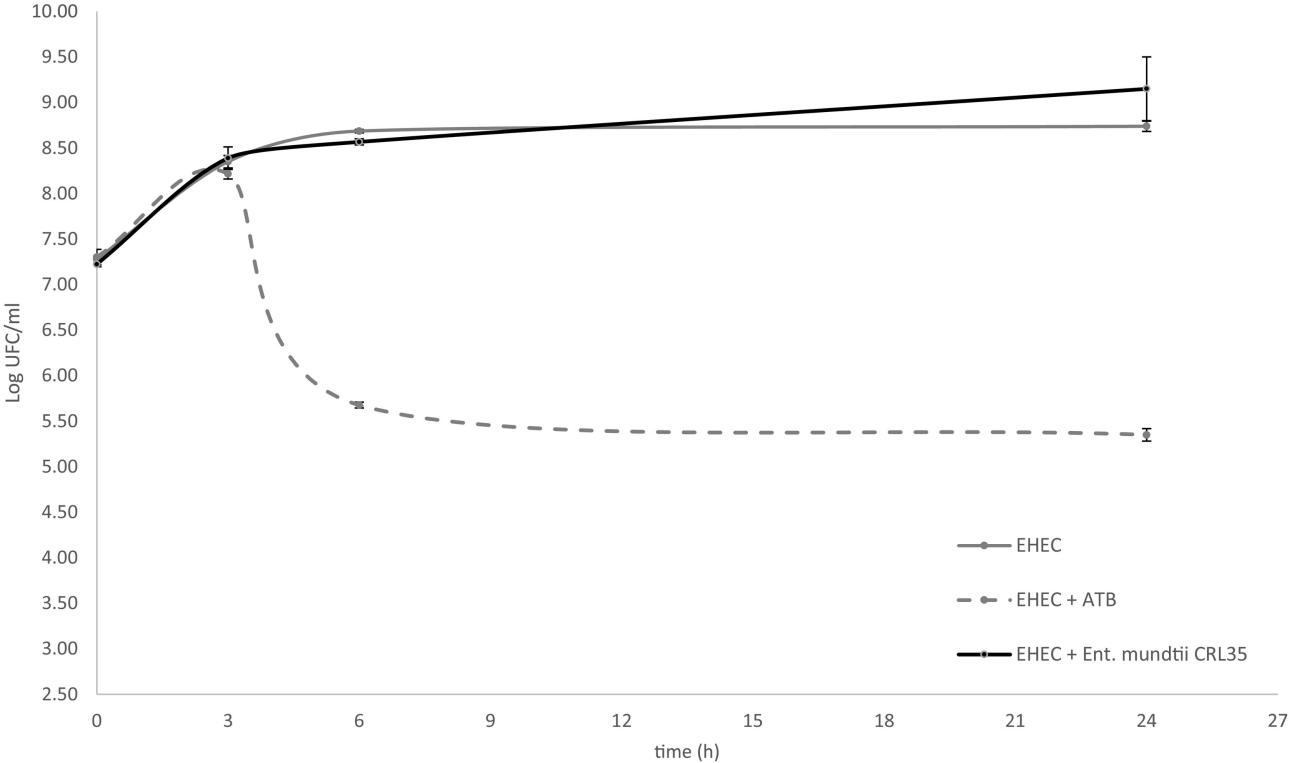
10.00
9.50
9.00
8.50
8.00
7.50
7.00
6.50
6.00
5.50
5.00
4.50
4.00
3.50
3.00
2.50
Log UFC/ml
0
3
6
9
12
15
18
21
24
27
time (h)
EHEC
EHEC + ATB
EHEC + Ent. mundtii CRL35

Figure 7